Omicron (B.1.1.529) - A new heavily mutated variant: Mapped location and probable properties of its mutations with an emphasis on S-glycoprotein

Chiranjib Chakraborty [a],[*],[1], Manojit Bhattacharya [b],[1], Ashish Ranjan Sharma [c],[1], Bidyut Mallik [d]

[a] Department of Biotechnology, School of Life Science and Biotechnology, Adamas University, Kolkata, West Bengal 700126, India
[b] Department of Zoology, Fakir Mohan University, Vyasa Vihar, Balasore 756020, Odisha, India
[c] Institute for Skeletal Aging & Orthopaedic Surgery, Hallym University-Chuncheon Sacred Heart Hospital, Chuncheon-si 24252, Gangwon-do, South Korea
[d] Department of Applied Science, Galgotias College of Engineering and Technology, Knowledge Park-II, Greater Noida, Uttar Pradesh 201306, India

ARTICLE INFO

ABSTRACT

Omicron, another SARS-CoV-2 variant, has been recorded and reported as a VoC. It has already spread across >30 countries and is a highly mutated variant. We tried to understand the role of mutations in the investigated variants by comparison with previous characterized VoC. We have mapped the mutations in Omicron S-glycoprotein's secondary and tertiary structure landscape using bioinformatics tools and statistical software and developed different models. In addition, we analyzed the effect of diverse mutations in antibody binding regions of the S-glycoprotein on the binding affinity of the investigated antibodies. This study has chosen eight significant mutations in Omicron (D614G, E484A, N501Y, Q493K, K417N, S477N, Y505H G496S), and seven of them are located in the RBD region. We also performed a comparative analysis of the ΔΔG score of these mutations to understand the stabilizing or destabilizing properties of the investigated mutations. The analysis outcome shows that D614G, Q493K, and S477N mutations are stable mutations with ΔΔG scores of 0.351 kcal/mol, 0.470 kcal/mol, and 0.628 kcal/mol, respectively, according to DynaMut estimations. While other mutations (E484A, N501Y, K417N, Y505H, G496S) showed destabilizing results. The D614G, E484A, N501Y, K417N, Y505H, and G496S mutations increased the molecular flexibility of S-glycoprotein to interact with the ACE2 receptor, increasing the variant's infectivity. Our study will contribute to research on the SARS-CoV-2 variant, Omicron, by providing information on the mutational pattern and exciting properties of these eight significant mutations, such as antibody escape and infectivity quotient (stabilizing or destabilizing; increased or decreased molecular flexibility of S-glycoprotein to interact with the human ACE2 receptor).

1. Introduction

Presently, SARS-CoV-2 variants have been a leading concern for public health, and these variants have made the pandemic more devastating [1]. Several variants have developed during the last one and a half years. Among them, some variants are termed VoC (variants of concern) and a few other variants as VoI (variants of interest) by WHO, CDC, and ECDC [1,2]. Some of the VoC are B.1.1.7 (Alpha variant), B.1.617.2 (Delta variant), B.1.351 (Beta variant), and P.1 (Gamma variant). Similarly, VoI are B.1.427/B.1.429 (Epsilon variant), B.1.526 (Eta variant), B.1.525 (Kappa variant) etc. [3]. It has been observed that every variant has its particular country of origin (Table 1). The first virulent VoC discovered was Alpha, which probably emerged in

September 2020 in the UK. Subsequently, it circulated throughout the UK and was responsible for a highly contagious wave. The geographical location might play a substantial role in the evolution of viral variants. Some studies have been performed to understand the association between the geographical location and the origin of SARS-CoV-2 variants [4–6]. Goyal et al. analyzed the SNP level of SARS-CoV-2 variants and found that allelic variants might be significantly associated with geographic origin. The inference was made from 692 genome sequence analysis of SARS-CoV-2 [7].

Remarkably, these variants originated rapidly, as this virus contains RNA as its genome. RNA viruses tend to evolve quicker compared to DNA viruses [8]. Therefore, SARS-CoV-2 is mutating rapidly like other RNA viruses [9]. A few months ago, researchers reported the dominancy

Table 1
Significant SARS-CoV-2 variants, their lineages, and first documented country.

Sl No.	Significant SARS-CoV-2 variants	Variants name (WHO label)	SARS-CoV-2 lineages	First documented country
1.	21K, GR/484A	Omicron	B.1.1.529	Multiple countries, as November-2021
2.	20I/501Y.V1	Alpha	B.1.1.7	United Kingdom
3.	21A, 21I, 21J/20A/S:478K	Delta	B.1.617.2	India
4.	20J/501Y.V3	Gamma	P.1	Brazil
5.	20J	Zeta	P.2	Brazil
6.	20H/501Y.V2	Beta	B.1.351	South Africa
7.	20C/S:452R	Epsilon	B.1.427/B.1.429	USA
8.	21D, G/484K.V3	Eta	B.1.525	USA
9.	21F, GH/253G.V1	Iota	B.1.526	USA

of the Delta variant, which became dominant by replacing existing variants [10]. Interestingly, the frequency of spread of the Delta variant increased worldwide.

Unexpectedly, a new variant has emerged in South Africa, entitled Omicron (B.1.1.529). In no time, it is being reported and isolated in several countries. WHO designated the Omicron variant as VoC on November 26, 2021, and it is the fifth one to be termed as VoC [11].

It has been found that the S-glycoprotein is critical for the pathogenesis of SARS-CoV-2. It is well known that the S-glycoprotein of SARS-CoV-2 interacts with the ACE2 receptor of the host cell for entering the cell [12,13]. Therefore, S-glycoprotein is critical for the access of virus to the host cell. Moreover, most of the available COVID-19 vaccines are based on S-glycoprotein (due to antigenicity) [14,15]. Several scientists have tried to explore the structural-functional and interaction properties of the SARS-CoV-2 S-glycoprotein from time to time. Researchers have explored the SARS-CoV-2 S-glycoprotein structure and its antigenicity. Walls et al. studied how S-glycoprotein utilizes the ACE2 receptor to enter the human host cells [16]. SARS-CoV-2 entry factors play a key role and have been studied through single-cell RNA expression maps by numerous researchers [17]. SARS-CoV-2 S-glycoprotein conformational changes and the flexibility of the trimeric spike protein play a crucial role in interactions with ACE2. These interactions are responsible for SARS-CoV-2 virulence and transmissibility. Recently, Mercurio et al. found that S-glycoprotein conformational changes are responsible for strong interactions with ACE2 and antibodies [18]. Wrapp et al. have developed a spike-trimer structure in the prefusion conformation to understand the S-glycoprotein conformational changes in a more detailed way. In this study, the researchers have developed a 3.5- Å -resolution structure through cryo-electron microscopy [19]. Tragni et al. developed 3D comparative models of the SARS-CoV-2 S-glycoprotein to evaluate how the SARS-CoV-2 Spike interacts with the ACE2 in the presence of emerging mutations such as E484K, N501Y, K417N. This study also evaluated the interaction energy at the RBD/ACE2 protein-protein interface [20]. Our research has also characterized these significant mutations (E484K, N501Y, K417N). Scientists are developing nanobodies for the therapy of COVID-19 [21]. They have tried to understand how the nanobodies interact with the S-glycoprotein. For this purpose, researchers have developed the COVID-19 Syrian golden hamster model and evaluated the interaction of S-glycoprotein with nanobodies [22]. Recently scientists found that three hinges are significant for S-glycoprotein flexibility [23]. Pierri commented that the flexibility of the S-glycoprotein might be an essential target in fighting against SARS-CoV-2 [24]. In this study, we have also tried to understand how mutations in the RBD of Omicron influence the flexibility of the S-glycoprotein.

The occurrence of mutations in S-glycoprotein is one of the critical parameters which might assist in changing the vital characteristic of the virus. Some mutations in S-glycoprotein are associated with immune escape, transmissibility, and infectivity. Altogether, mutations in S-

glycoprotein are also related to antigenicity and pathogenicity [1,25]. It has been observed that missense mutations on S-glycoprotein affect its receptor-binding affinity and stability. Teng et al. have observed that mutations located on the RBD of the S-glycoprotein can affect RBD-ACE2 interactions. SARS-CoV-2 close residues (G496 and F497) and ACE2 residues (D355 and Y41) are crucial for RBD-ACE2 interactions [26]. Scientists have shown that D614G mutation in S-glycoprotein affects the cleavage pattern of S-glycoprotein, infection, and re-infection [9,27]. Therefore, it is essential to understand the role of mutations in S-glycoprotein, which might provide factual information about the altered infection efficiency of the investigated variants. Consequently, it is also urgent for us to understand the role of the S-glycoprotein mutations in the infections from the emerging Omicron variant.

It has been noted that vaccination might elicit neutralizing antibodies (nAb), protecting individuals and populations against the virus. In SARS-CoV-2 infection, nAb targets S-glycoprotein for neutralizing the viral ability to enter the host cells [12,28,29]. Due to mutations in different positions of the S-glycoprotein, several variants have acquired the ability to escape antibodies [29–35]. For example, it has been found that the mutations in different positions of the S-glycoprotein in the Delta variant are responsible for the reduced neutralization properties of antibodies. In this direction, Planas et al. performed one study to comprehend the effects of mutations of Delta variants on clinically approved monoclonal Abs and other monoclonal Abs. The researchers used four monoclonal Abs such as imdevimab (REGN10987), casirivimab (REGN10933), etesevimab (LY-CoV016), bamlanivimab (LY-CoV555), and eight other monoclonal Abs (anti-RBD and anti-NTD monoclonal Abs). T478K mutation is a Delta variant-specific mutation. This mutation is associated with the epitope region, which might be involved in interactions with neutralizing mAbs. The study found that T478K is close to mutation E484K and associated with antibody escape. Simultaneously, the study observed that the variant was resistant to some antibodies, including bamlanivimab, anti-RBD, and anti-NTD monoclonal Abs [36].

Vaccination-induced Delta variant neutralization was less effective than previous early Wuhan virus neutralization [37]. The mutations in the Delta variant were shown to reduce the efficacy of vaccines [38]. Thus, the mutations in all the variants have an immense role in lowering the neutralization of different antibodies. Thus, it is necessary to understand the role of Omicron spike mutations in antibody escape/resistance.

Our study aims to shed light on the role of Omicron spike mutations in infectivity, also by comparison with mutations characterized in other VoC. In this direction, our first objective was to understand the role played by mutations in the secondary structure and tertiary structure landscape of S-glycoprotein in Omicron. The second objective was to figure out the role played by mutations in antibody (nAb) binding regions or the mutations in adjacent antibody (nAb) binding regions of the S-glycoprotein of the variants. The third objective was to portray the noteworthy characteristics of the eight crucial mutations (D614G, E484A, N501Y, Q493K, K417N, S477N, Y505H, and G496S) of the Omicron variant relating to stabilizing or destabilizing properties. Moreover, we also tried to analyze the increased or decreased molecular flexibility of S-glycoprotein to understand the effect of mutations on interactions with the ACE2 receptor.

2. Methods

2.1. Data collection for Omicron variant to understand the mutational landscape

We collected the latest information on the variants of SARS-CoV-2 using Google Scholar [39], PubMed [40,41], and Web of Science [42]. The study retrieved/ collected data on the Omicron variants from the CDC [43,44]; eCDC [45] and WHO [46]. Keywords such as "Omicron variant" and "B.1.1.529" were used to find the genomic information,

and different data were retrieved from the open resource part of the GISAID database [47,48]. The COVID-19 data was also gathered from several countries and Nextstrain [49]. Nextstrain SARS-CoV-2 resources are available on Nextstrain [50]. We collected the PDB file of S-glycoprotein in an open state and S-glycoprotein-antibody interaction from the RCSB-PDB database [51].

2.2. Data analysis and interpretation for Omicron variant to understand the mutational landscape

2.2.1. Understanding the Omicron mutation in secondary structure landscape

In this part of the study, we used the PdbSum server to understand mutations in the secondary structure landscape of S-glycoprotein in Omicron [52]. At the same time, the server developed the sequence Logo to evaluate the conserved amino acid of the regions of the S-glycoprotein.

2.2.2. The prediction of the characteristic mutations (changed flexibility and stability etc.) on S-glycoprotein of Omicron

The DynaMut server analyzed the mutations on S-glycoprotein and its characteristic effect on the Omicron variant [53]. The server analyzed the mutation properties, such as increasing or decreasing molecular flexibility and stabilizing or destabilizing events. The interatomic interactions, fluctuation, and deformation analysis of an amino acid mutation can be illustrated through Delta-Delta G ($\Delta\Delta G$). We have calculated the $\Delta\Delta G$ score of the point mutations of the Omicron S-glycoprotein to describe its stability (thermodynamic stability). It has been noted that the server illustrated the point mutation into two categories, such as stabilizing or destabilizing events. The point mutation is described as stabilizing event when the $\Delta\Delta G$ score was noted as ≥ 0. Similarly, the mutation was described as destabilizing when $\Delta\Delta G$ score was reported as < 0 [53]. Other researchers have demonstrated the similar score of the $\Delta\Delta G$ for stabilizing or destabilizing events [54].

In this study, we have analyzed $\Delta\Delta G$ ENCoM, where we examined the $\Delta\Delta G$ score point mutation using ENCoM. ENCoM is an Elastic Network Contact Model calculated through a different NMA approach called the "coarse-grained NMA method." It tries to measure the consequence of the particular property of amino acids on dynamics using a potential energy function. During calculation, a pairwise atom-type non-bonded interaction expression was also considered [53,55]. At the same time, we also analyzed different structure-based predictions such as $\Delta\Delta G$ mCSM, $\Delta\Delta G$ SDM, and $\Delta\Delta G$ DUET.

Here, we have also calculated $\Delta\Delta G$ mCSM, where the $\Delta\Delta G$ score of point mutation was analyzed using mCSM. mCSM (mutation Cutoff Scanning Matrix) is measured to investigate the atomic-distance patterns of missense mutations [53,56].

$\Delta\Delta G$ of the point mutation was calculated by using SDM. The SDM (Site Directed Mutator) is a potential energy function derived from the statistical calculation, and it analyzes stability scores. During analysis, the method uses amino-acid substitution frequency and it is calculated an analogous free energy difference between the wild-type protein and mutant-type protein [53,56,57].

$\Delta\Delta G$ DUET was also evaluated where we calculated the $\Delta\Delta G$ score of point mutation. DUET uses two approaches (SDM and mCSM) for the prediction. Finally, the two results have been combined and optimized using SVM (Support Vector Machines) [53,58].

We also calculated the $\Delta\Delta S$VibENCoM (vibrational entropy energy), providing information about the vibrational entropy changes between the wild type and the mutant type. It helps to understand the vibrational entropy energy and its effects on protein stability due to single-point mutation [53,59]. During $\Delta\Delta G$ calculations, the DynaMut server used the Wuhan strain as the reference value. Conversely, it has been noted that proteins are dynamic in nature with rapid conformational fluctuations or alternation. These conformational alternations can be measured by the DynaMut server evaluated using NMA [53].

2.2.3. Statistical models, plots, and graphs

Statistical models were generated using statistical software (PAST 4.03 software) [60]. Similarly, MATLAB was also used to analyze the plots and graphs [61].

Moreover, we have depicted a flow diagram to provide a bird's eye view of our study to understand the mutational landscape of the Omicron (B.1.1.529) variant (Fig. 1a). Also, the location of the selected eight mutations from the S-glycoprotein for our study has been depicted (Fig. 1b).

3. Results

3.1. Mapping the mutations in the Omicron variant and comparison of mutations with other VoC

We have extensively studied the mutations in Omicron throughout the genome, and several mutations were recorded in protein-coding genes. The observed Omicron mutations in the structural and non-structural proteins are recorded in Table S1 and are schematically represented through a diagram (Fig. 2A). Similarly, we have also observed the number of mutations in different structural proteins (S, E, M, and N) and non-structural proteins (nsp3, nsp4, nsp5, nsp6, nsp12, and nsp14). A statistical model was developed using the number of mutations of structural and non-structural proteins (Fig. 2B). The maximum number of mutations was observed in the S protein. Meanwhile, a minimum number of mutations were in one structural protein and four non-structural proteins (E and nsp4, nsp5, nsp12, nsp14, respectively).

Next, detailed mutation analysis of the S-glycoprotein of Omicron was performed. Several mutations in different regions of the S1 and S2 subunits of S-glycoprotein were recorded (Fig. 2C). In addition, our analysis noted many mutations in several other areas in the S-glycoprotein of Omicron. A model was developed using the number of mutations (Fig. 2D). The maximum number of mutations was observed in the RBD region of the S-glycoprotein. Concurrently, the minimum number of mutations was in two S-glycoprotein regions (FP regions and regions 806 to 912). The second-highest number of mutations was noted in the NTD.

The total number of mutations in Omicron was compared with the mutations of other VoC (Delta, Gamma, and Alpha) (Fig. 2E). Our analysis found maximum mutations in Omicron and minimum in Alpha. Similarly, we found the total number of mutations in the S-glycoprotein in Omicron and other VoC (Delta, Gamma, and Alpha) (Fig. 2F). The analysis noted a maximum number of mutations in the S-glycoprotein of Omicron and a minimum in the S-glycoprotein of Alpha. In both cases, the number of Omicron mutations is higher than the other VoCs.

3.2. Mapping the mutations in the secondary structure landscape of S-glycoprotein in Omicron

We next analyzed the effect of mutations in the secondary structure landscape of S-glycoprotein in Omicron. For this, secondary structure components like α-helix and the β-sheet in different regions of the S-glycoprotein in Omicron were analyzed. Simultaneously, the conserved residues in each position through the sequence Logo were analyzed. The secondary structure components and conserved residues are illustrated in NTD (Fig. 3A and Fig. 3B), RBD (Fig. 3C and Fig. 3D), and HR1 (Fig. 3E and Fig. 3F). We analyzed mutations in RBD that were located in the β-sheet regions and other regions. We observed that mutation A67V was present in the β-sheet area.

Similarly, Δ69-70 was found in NTD (which was also shared with the Alpha variant spike) [62]. In comparison, Δ143-145 was found situated in a β-sheet area. The conserved residues from the sequence logo illustrate mutations in less conserved regions, and the generated sequence logo from NTD shows a similar kind of result. The mutation A67V, Δ69-70, indicates relative frequency and implies that mutations occur in the less conserved region.
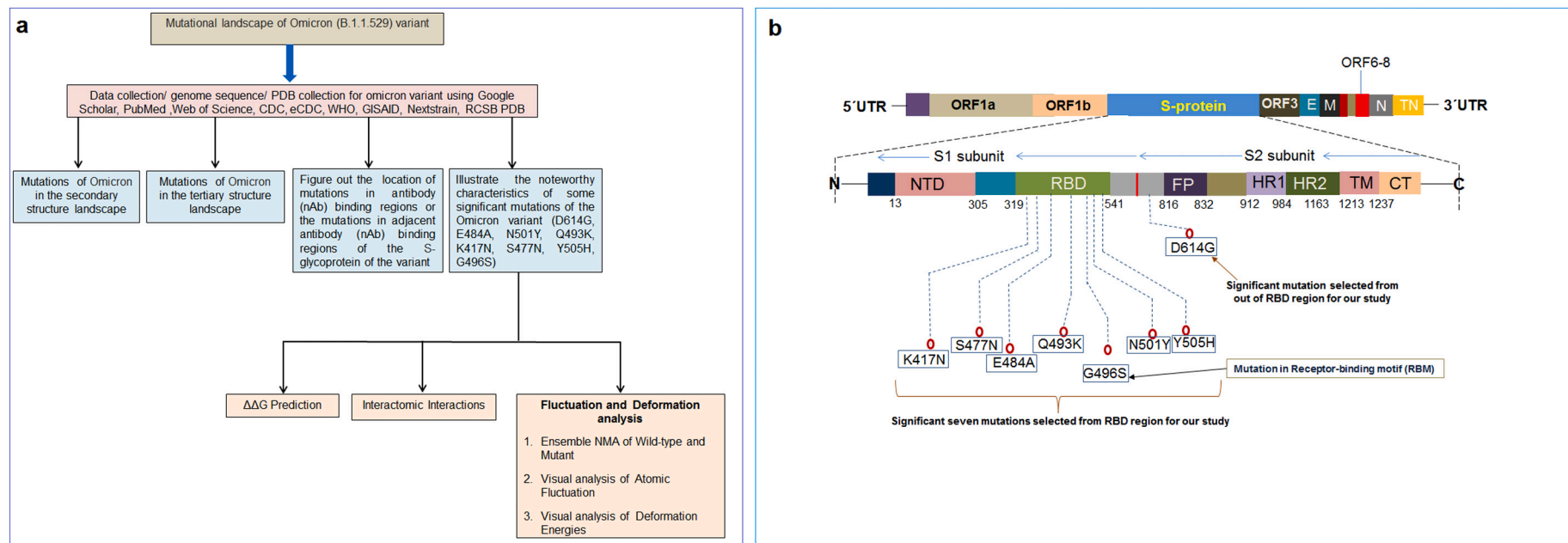
Fig. 1. The flow diagram of our comprehensive study and a schematic diagram shows the location of the mutations selection in our study. (a) A flow diagram of our study to evaluate the mutational landscape of the Omicron (B.1.1.529) variant. (b) A schematic diagram shows the location of the selected eight mutations from the S-glycoprotein for our study. The diagram illustrates that seven mutations were selected from the RBD region, and one mutation was selected from outside the RBD region (D614G).
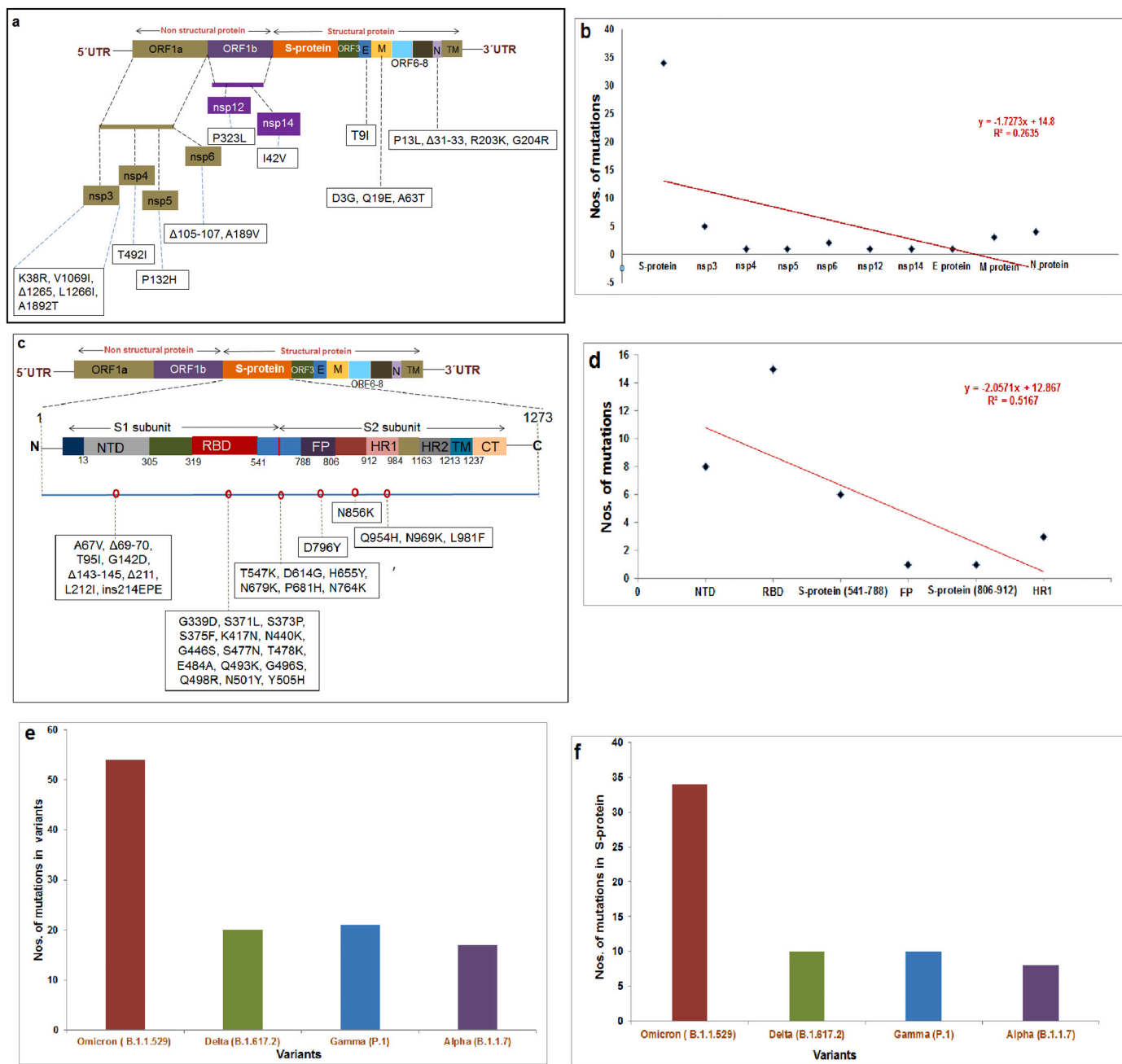
Fig. 2. Mapped mutations in the Omicron variant. (a) The schematic diagram shows mutations in structural proteins (S, E, M, and N) and non-structural proteins (nsp3, nsp4, nsp5, nsp6, nsp12, and nsp14). (b) A statistical model using the number of mutations in structural and non-structural proteins. (c) The schematic diagram shows mutations in the different regions of the S1 and S2 subunits in the S-glycoprotein in Omicron. (d) A statistical model using the number of mutations in the different areas of the S1 and S2 subunit of S-glycoprotein. (e) Comparing mutations in Omicron and other VoC (Delta, Gamma, Alpha), considering structural and non-structural proteins. (f) Comparing mutations in Omicron and other VoC (Delta, Gamma, Alpha), considering S-glycoprotein.

The analysis revealed that mutations in RBD were located in the β-sheet or α-helix or excluding this region. The mutations K417N and N440K were found in different α-helix areas. Meanwhile, S375F was found in a β-sheet area and Q493K in another β-sheet region. Conversely, the mutation G446S was found other than the β-sheet or α-helix. The RBD mutations were present in the less conserved regions. Fig. 3D depicts the presence of mutations G339D, S373P, and S375F in the less conserved region of RBD.

Mutations in HR1 were located in the α-helix regions. The mutations D950N and Q954H were found in the same α-helix areas. In contrast, N969K was located in regions excluding the α-helix/β-sheet.

3.3. Mapping the mutations in the tertiary structure landscape of S-glycoprotein in Omicron

The mutations in Omicron were mapped in the tertiary structure space of S-glycoprotein in Omicron. We found that all the mutations are randomly distributed in the S-glycoprotein along with the RBD regions (Fig. 4A). We mapped >15 noteworthy mutations in RBD regions of the S-glycoprotein of Omicron. At the same time, we also mapped mutations in the RBM area (Fig. 4B). About 10 important mutations were noted in the RBM area. Some significant mutations are N440K, T478K, Q493K, Q498R, N501Y, and Y505H. Several new mutations were found in the S-glycoprotein of Omicron compared to other VoC (Table 2). We noted
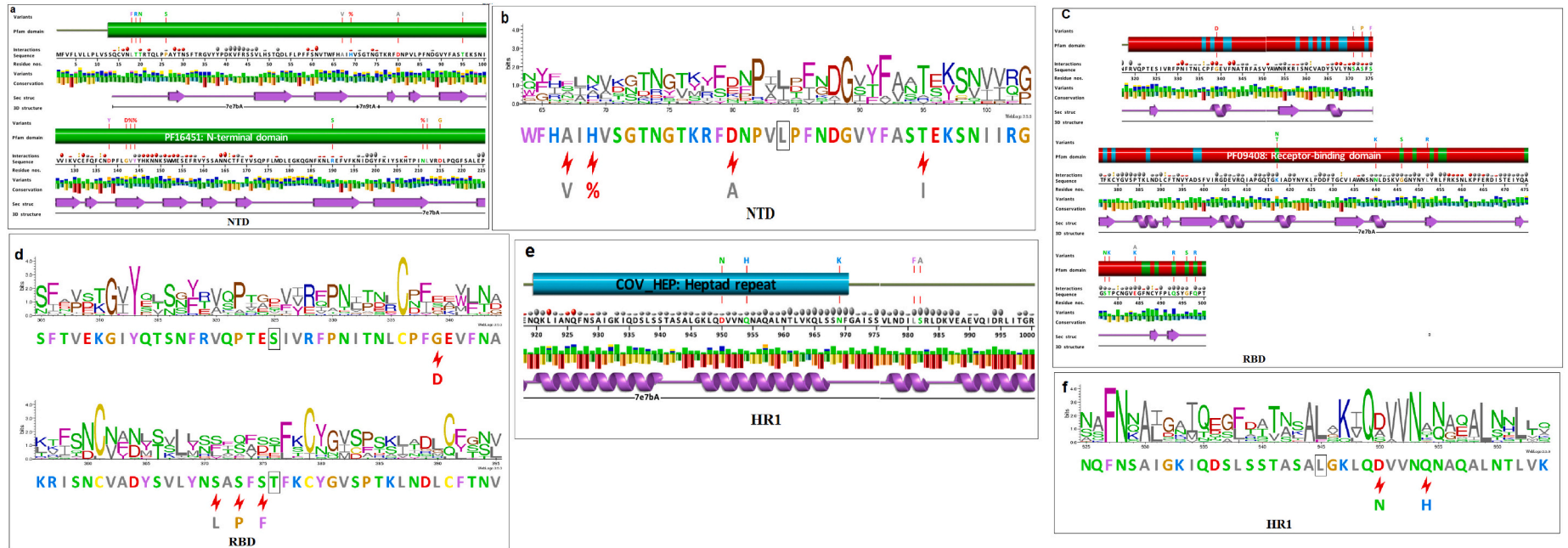
Fig. 3. Mapped mutations in the secondary structure landscape of S-glycoprotein in Omicron. (a) Mutations in the N-terminal domain (NTD), considering the secondary structure. (b) Sequence Logo developed using NTD, which shows the sequence conservation in the residue of NTD. (c) Mutations in the receptor-binding domain (RBD), considering the secondary structure. (d) The sequence Logo developed using the RBD shows the sequence conservation in the residue of RBD. (e) Mutations in the receptor heptad repeat (HR1), considering the secondary structure. (f) Sequence Logo developed using heptad repeat (HR1) shows the sequence conservation in the residue of HR1.
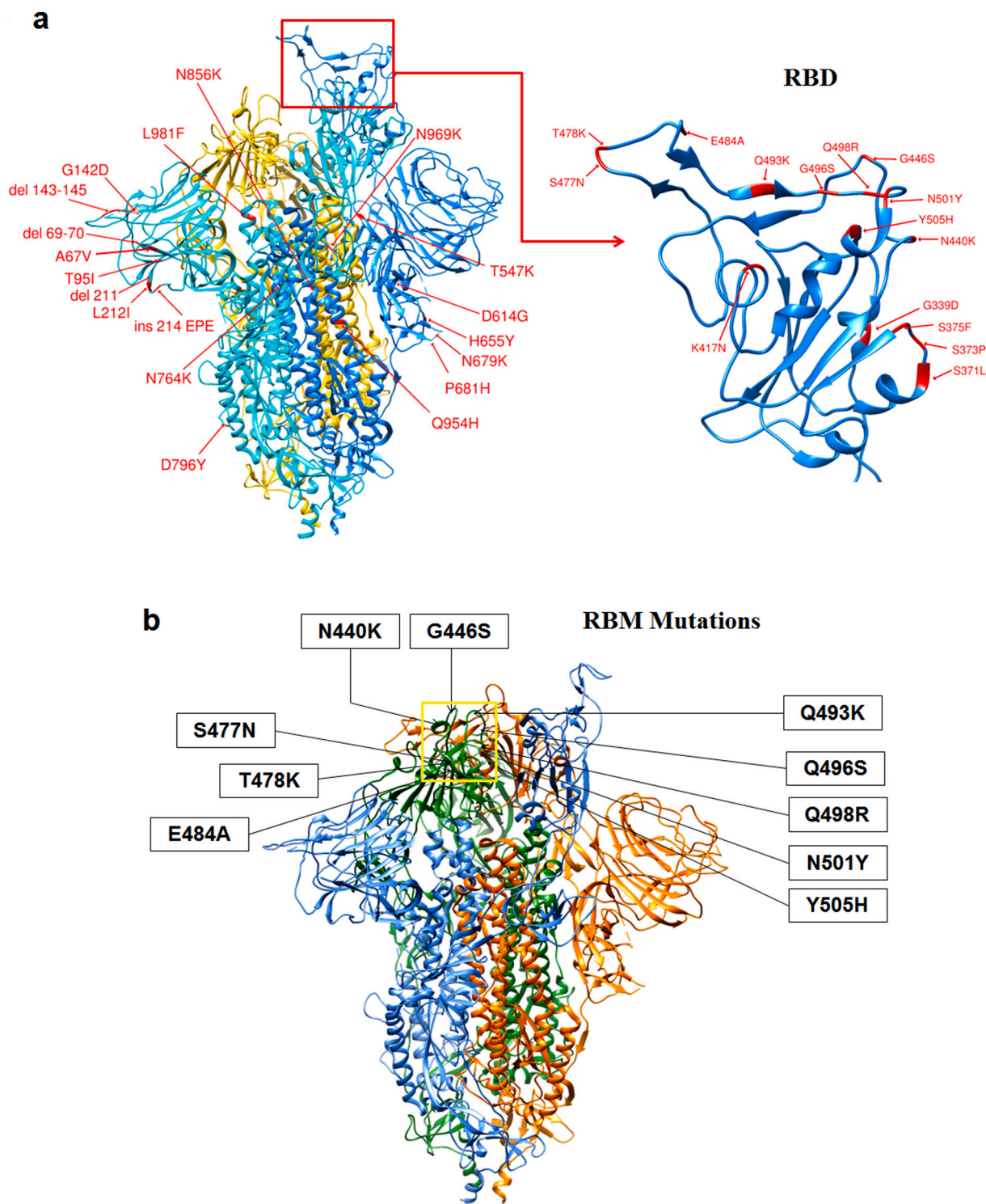
Fig. 4. Mapped mutations in the tertiary structure landscape of S-glycoprotein in Omicron. (a) Location of mutations in the tertiary structure landscape of S-glycoprotein highlighting RBD. (b) Location of mutations in the RBM in tertiary structure landscape of S-glycoprotein.

several novel mutations like S375F, S373P, S371L, G339D, N440K, G446S, S477N, Q493K, Q496S, Q498R, and Y505H compared to the Delta, Gamma, and Alpha variants.

3.4. Mapping the mutations in neutralizing antibody (nAb) binding regions of S-glycoprotein in Omicron

Presently, a big question is whether Omicron can escape antibodies or not. Scientists are analyzing the mutations responsible for antibody

escape and vaccine escape for SARS-CoV-2 [63,64]. nAb structure is vital for their interaction. According to the structure and their interaction properties, researchers have categorized nAb into four classes. Barnes et al. [65] have classified SARS-CoV-2 nAb into four classes. The first nAb class (Class-1) binds with the 'up' RBDs. This nAb contains a VH3-53 part with a short CDRH3 loop. The second nAb class (Class-2) binds with 'down' and 'up' RBDs. It usually binds nearby RBDs. The third nAb class (Class-3) can also bind with both 'down' and 'up' RBDs. However, it attaches outside the ACE2 region. The fourth nAb class

Table 2

Significant mutations within the S-protein of four SARS-CoV-2 variants; Omicron (B.1.1.529), Delta (B.1.617.2), Gamma (P.1), and Alpha (B.1.1.7).

Variants name	Mutations in Spike (S) glycoprotein	
	Other than RBD region	RBD region
Omicron (B.1.1.529)	A67V, Δ69–70, T95I, G142D, Δ143–145, Δ211, L212I, ins214EPE,T547K, D614G, H655Y, N679K, P681H, N764K, D796Y, N856K, Q954H, N969K, L981F	G339D, S371L, S373P, S375F, K417N, N440K, G446S, S477N, T478K, E484A, Q493K, G496S, Q498R, N501Y, Y505H
Delta (B.1.617.2)	G142D, T19R, R158G, D614G, P681R, D950N, E156del, F157del	L452R, T478K
Gamma (P.1)	L18F, T20N, P26S, D138Y, R190S, H655Y, T1027I	K417T, E484K, N501Y
Alpha (B.1.1.7)	HV 69–70 deletion, Y144 deletion, A570D, P681H, T716I, S982A, D1118H	N501Y

(Class-4) is similar to the first class of nAb. It is unable to block ACE2 and can only attach to 'up' RBDs. Following this classification, Greaney et al. have comprehended how SARS-CoV-2 RBD mutations are responsible for antibody escape. They found that the obtained E484K mutation at RBD is the most effective in the escape of class-2 antibodies [66]. They also found that RBD mutations decrease antibody binding efficiency at the interaction site.

In this direction, we analyzed the mutations in the S-glycoprotein's antibody binding regions in Omicron (Table 3). We considered the four antibody classes (Class-1, Class-2, Class-3, and Class-4) to understand the interaction residue position of the nAb and binding regions of S-glycoprotein. We noted mutations in the nAb binding regions or adjacent mutations in the interacting position. The general interaction of Class-1 nAb with S-glycoprotein is depicted in Fig. 5A. While, the general interaction of Class-2 nAb with S-glycoprotein is depicted in Fig. 5B. Similarly, another diagram mapped mutational position in the nAb binding regions or adjacent mutations in the nAb binding areas (Fig. 5C).

3.5. Mapping the significant properties of D614G, E484A, N501Y, Q493K, K417N, S477N, Y505H, G496S

In this analysis, we tried to understand the properties of some mutations (D614G, E484A, N501Y, Q493K, K417N, S477N, Y505H, G496S). ΔΔG scores, interatomic interactions, fluctuation, and deformation analysis were analyzed. ΔΔG score illustrates how point mutations change protein stability [67]. A deeper understanding of point mutation help to assess the interaction interfaces from the wild type to mutant type and might help evaluate the change in the interaction space of the protein-protein binding [68]. Fluctuation and deformation analysis provides information about the assembly by Normal Mode Analysis (NMA) of wild-type and mutant-type and depicts the RMS fluctuation of molecules [69].

#### 3.5.1. Mapping the properties of D614G

We analyzed ΔΔG score, interatomic interactions, and fluctuation and deformation analysis in the D614G mutation. The outcome of the analysis of ΔΔG score of D614G mutation is depicted in Fig. 6A. Here, the analysis calculated the outcome of ΔΔG score to be 0.351 kcal/mol. The NMA-based predictions show that ΔΔG ENCoM is −0.134 kcal/mol, which is destabilizing. Other structure-based predictions showed ΔΔG mCSM (−0.514 kcal/mol; destabilizing), ΔΔG SDM (2.510 kcal/mol; stabilizing) and ΔΔG DUET (0.171 kcal/mol; stabilizing). We analyzed Δ vibrational entropy energy between wild-type and mutant, which showed ΔΔSVib ENCoM as 0.168 kcal.mol^{-1}.K^{-1}. The outcome of the model predicts an increase in molecule flexibility. The interatomic interactions are shown in Fig. 6B (the wild-type and mutant residues are

Table 3

Mutation in antibodies interaction area within S-protein of Omicron variant. Here, we mapped the mutations in the residue of interaction with antibodies (nAbs) or the mutations in the adjacent area of interaction with antibodies (nAbs). It also illustrates the SARS-CoV-2 neutralizing antibodies (nAbs), their class, and PDB Id used in this study.

Sl No	Antibody name	Antibody class	PDB id	Amino acids residue and positions of S-glycoprotein that interact with neutralizing antibodies (nAbs)	Mutations in the residue of interaction with antibodies (nAbs) or the mutations in the residues of adjacent area of interaction with antibodies (nAbs)
1	BD-744 BD-813	Class-1	7EY0	E340, T345, R346, N354, Y449, N450, L452, R466, I468, T470, F490, L492	G339D, G446S, Q493K
				T415, D420, Y421, L455, F456, R457, N460, Y473, A475, S477, T478, F486, N487, Y489, Y505	K417N, S477N, T478K, E484K, Y505H
2	BG1-22	Class-1	7M6F	R408, D420, Y421, T415, A457, N460, A475, S477, F486, Q493, Y495, T500, V503,	K417N, S477N, E484A, Q493K, G496S, Q498R, V505H
3	P2B-1A10	Class-1	7CZQ	K417, Y449, L455, F456, A475, N487, Y489, Q493, G496, T500, N501, G502, Y505	K417N, G446S, S477N, Q493K, G496S, Q498R, N501Y, Y505H
4	13G9	Class-2	7E3K	Q493, E484, K458, S477, F486	E484A, Q493K, S477N
5	C548	Class-2	7R8O	L455, F486, Q498, F490, Q493, E484	E484A, Q493K, Q498R
6	C051	Class-2	7R8N	L455, Q493, S494	Q493K, G496S
7	C032	Class-3	7R8M	T345, R346, N440, L441, K444, V445, N448,	N440K, G446S
8	47D11	Class-3	7AKD	F338, F342, Y365, V367, L368, F374	G339D, S373P, S375F
9	BG10-19	Class-3	7M6E	V445, Y489, F490, Q498, N343, F374, N450, N440, L441, R346, W436, V367	G446S, Q493K, G496S, Q498R, S373P, N440K
10	C118.	Class-4	7RKV	L355, Y365, F364, C366, G391, D392, V394, K417, F416, D415, D414, P399. G400, Q401, T402	K417N
11	S2X259	Class-4	7RA8	Y369, C379, K378, F377, T385, S383, Y380, R408, D405	S371L, S375F
12	5A6	Class-4	7M71	D471, N481, E484, Y489, F490, N487, F486	E484A, Q493K

colored in light green). It also illustrates the adjacent residues involved in any interaction. The fluctuation of the wild-type and mutant residues were also observed (Fig. S1A). More fluctuation was noted in mutant residues compared to the wild-type proteins. The maximum fluctuation
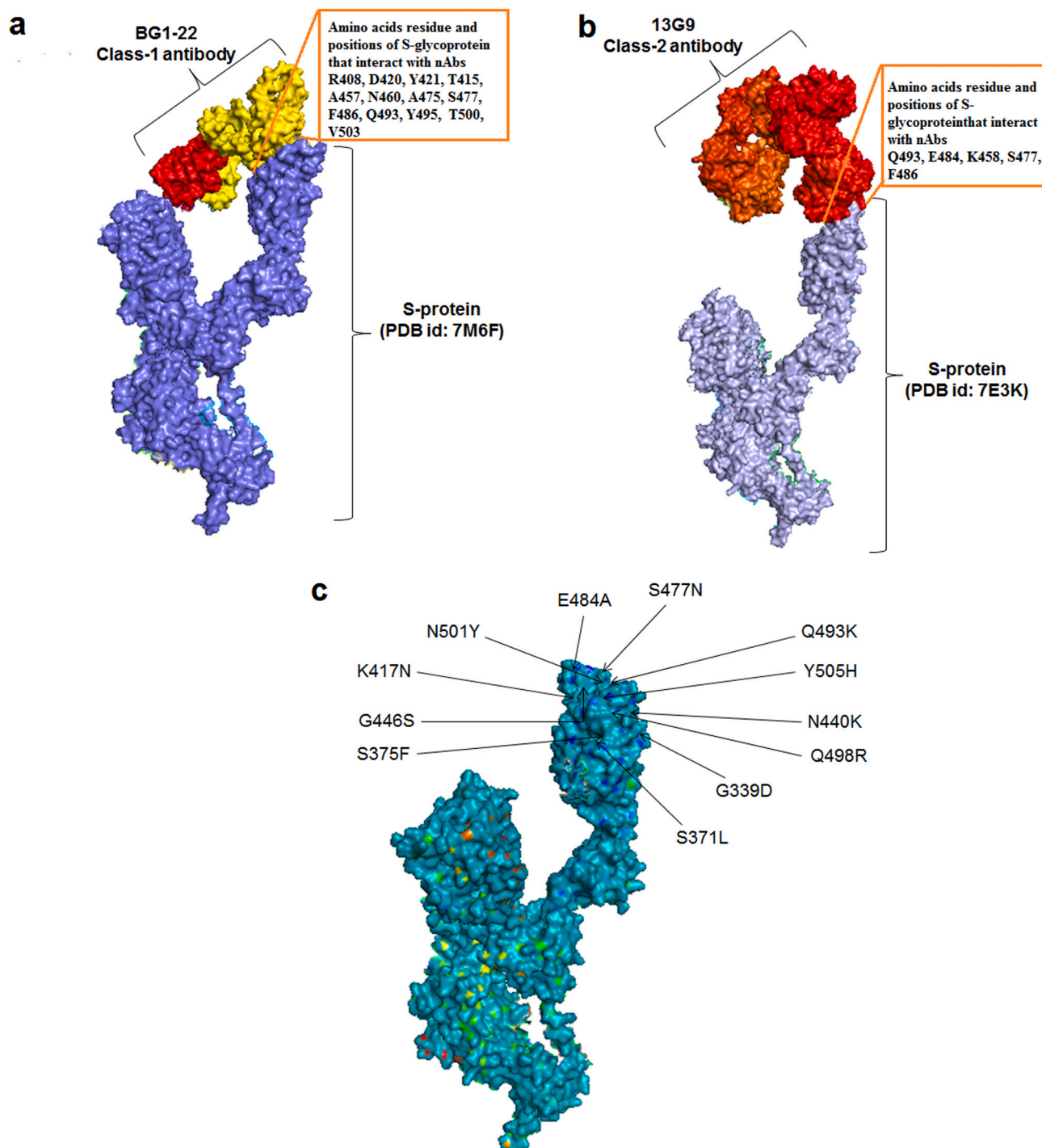
Fig. 5. Spotted mutations in the antibody (nAb) binding regions of S-glycoprotein in Omicron. (a) BG1–22 antibody (Class-1 antibody) and its interaction with S-glycoprotein show the residues involved in this interaction. (b) 13G9 antibody (Class-2 antibody) and its interaction with S-glycoprotein show the residues involved in this interaction. (c) Predicted mutation position in the nAb binding regions or adjacent mutations in the nAb binding areas.

was noted in residues between 400 and 500, nearer to residue number 700, and after 1000. Visual analysis of atomic fluctuations shows the atomic fluctuations of the 3D space of S-glycoprotein, both in the wild and mutant types (Fig. S1B). The maximum atomic fluctuations were noted in the terminal position. Simultaneously, we analyzed the visual analysis of deformation energies to show the amount of local flexibility of the 3D space of S-glycoprotein, both in the wild and mutant types (Fig. S1C). Like the previous outcome, a maximum amount of flexibility was noted in the terminal position.

3.5.2. Mapping the properties of E484A

Next, the $\Delta\Delta G$ of E484A mutation was evaluated (Fig. 7A). The observed score was -0.456 kcal/mol. We found that $\Delta\Delta G$ ENCoM is -0.377 kcal/mol (destabilizing). The other structure-based analyses showed three parameters i) $\Delta\Delta G$ mCSM as -0.415 kcal/mol, destabilizing; ii) $\Delta\Delta G$ SDM as 0.320 kcal/mol, stabilizing and iii) $\Delta\Delta G$ DUET as -0.128 kcal/mol, destabilizing. The analyzed Δ vibrational entropy energy between wild and mutant types was noted as $\Delta\Delta$SVib ENCoM (0.471 kcal.mol^{-1}.K^{-1}). The result shows an increase in molecule flexibility. Simultaneously, the interatomic interactions of E484A were
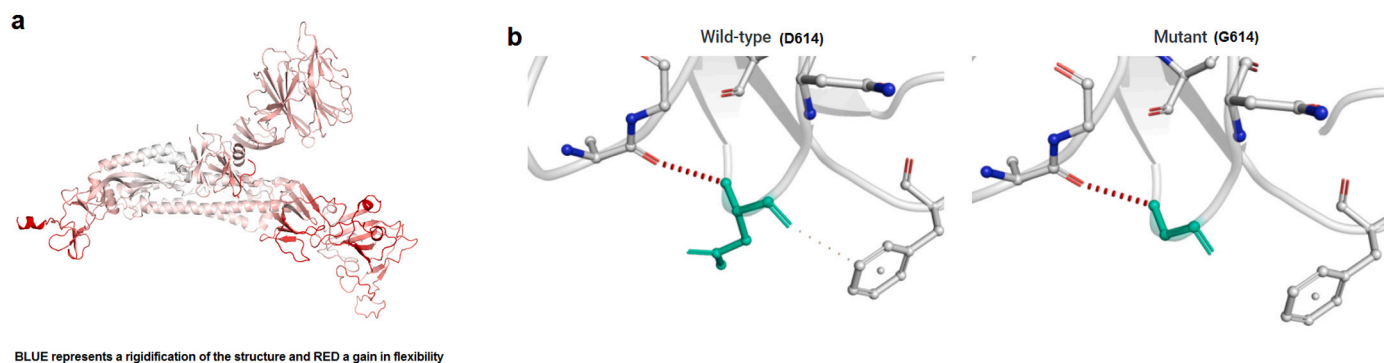
Fig. 6. Illustrated significant properties of D614G. (a) Vibrational entropy energy of D614G with a visual representation through ΔΔG score prediction. (b) Interatomic interactions of wild type to mutant type D614G mutation.
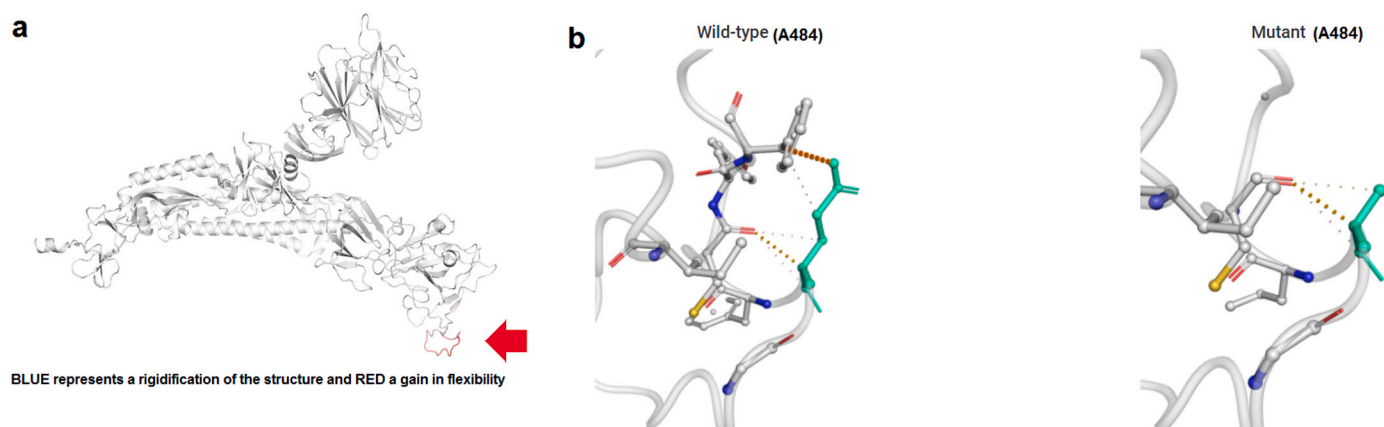
Fig. 7. Mapped important properties of E484A. (a) Vibrational entropy energy of E484A with a visual representation through ΔΔG score prediction. (b) Interatomic interactions of wild type to mutant type E484A mutation.
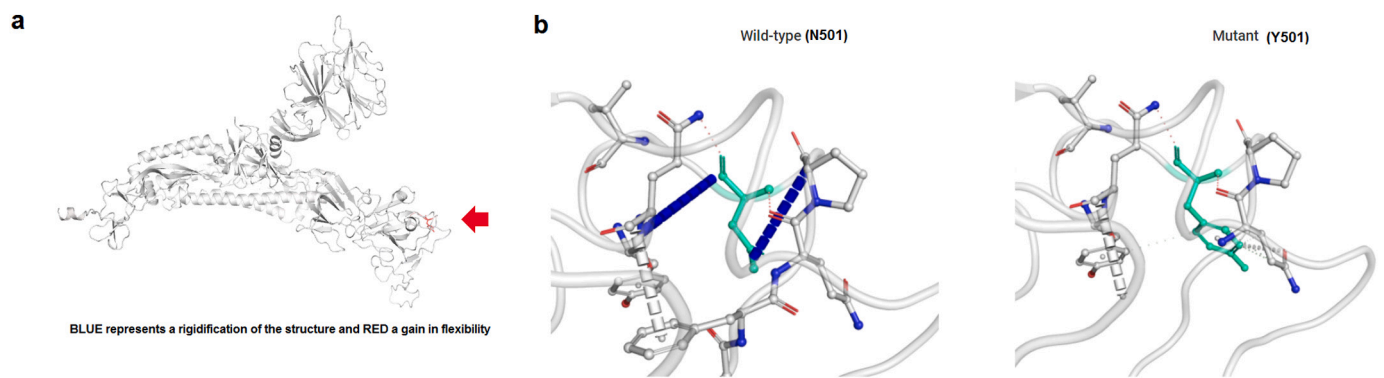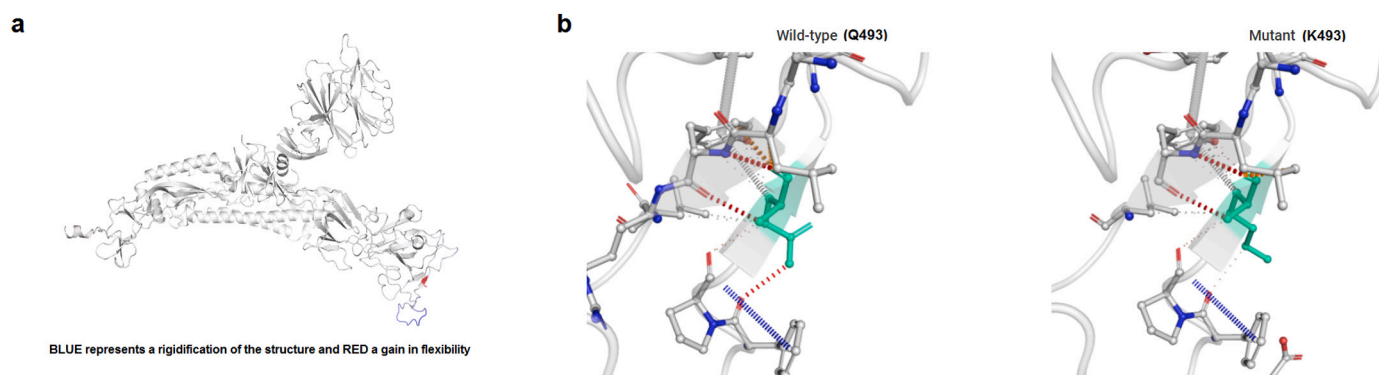

Fig. 8. Evaluated significant properties of N501Y. (a) Vibrational entropy energy of N501Y with a visual representation through ΔΔG score prediction. (b) Interatomic interactions of wild type to mutant type N501Y mutation.

observed for wild- and mutant-type residues (Fig. 7B) and adjacent residues involved in the interaction. The fluctuation of the wild and mutant-type residues were also recorded (Fig. S2A). More fluctuation was noted in mutant-type residues compared to the wild-type. A similar fluctuation was noted during the analysis of deformation energy in E484A mutation. The atomic fluctuations in the virtual model of the 3D space of S-glycoprotein (the wild-type and mutant-type) are depicted in Fig. S2B. In this mutation, the maximum atomic fluctuations were noted in the terminal area of the S-glycoprotein. Also, the visual analysis of deformation energies was observed for the 3D space of S-glycoprotein in the wild and mutant types (Fig. S2C).

3.5.3. Mapping the properties of N501Y

We observed the ΔΔG of N501Y mutation and noted it as −0.203 kcal/mol (Fig. 8A). ΔΔG ENCoM of N501Y was −0.094 kcal/mol, which is destabilizing. We again evaluated the structure-based other parameters for N501Y mutation like ΔΔG mCSM (−0.457 kcal/mol, destabilizing); ΔΔG SDM (0.280 kcal/mol, stabilizing); and ΔΔG DUET (−0.471 kcal/mol, destabilizing). At the same time, Δ vibrational entropy energy among wild and mutant types was also observed (ΔΔSVib ENCoM as 0.117 kcal.mol^{-1}.K^{-1}). The results display enhanced molecule flexibility. Other analyses revealed the interatomic interactions of N501Y mutation for wild and mutant-type concerning residues and their interaction with nearby residues (Fig. 8B). The fluctuations of residues were also observed for the wild and mutant-type residues (Fig. S3A). A

Fig. 9. Mapped noteworthy properties of Q493K. (a) Vibrational entropy energy of Q493K with a visual representation through ΔΔG score prediction. (b) Interatomic interactions of wild type to mutant type Q493K mutation.
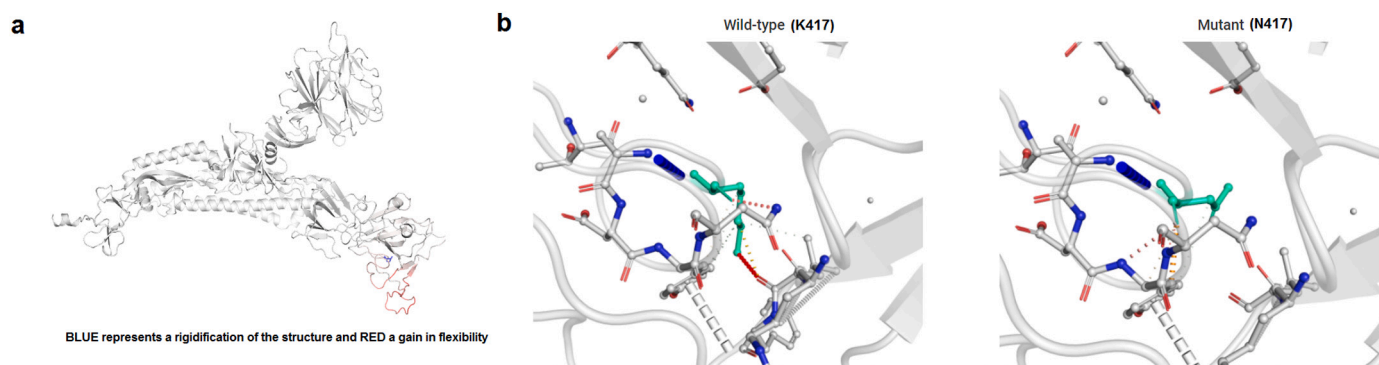
Fig. 10. Illustrated significant properties of K417N. (a) Vibrational entropy energy of K417N with a visual representation through ΔΔG score prediction. (b) Interatomic interactions of wild type to mutant type K417N mutation.
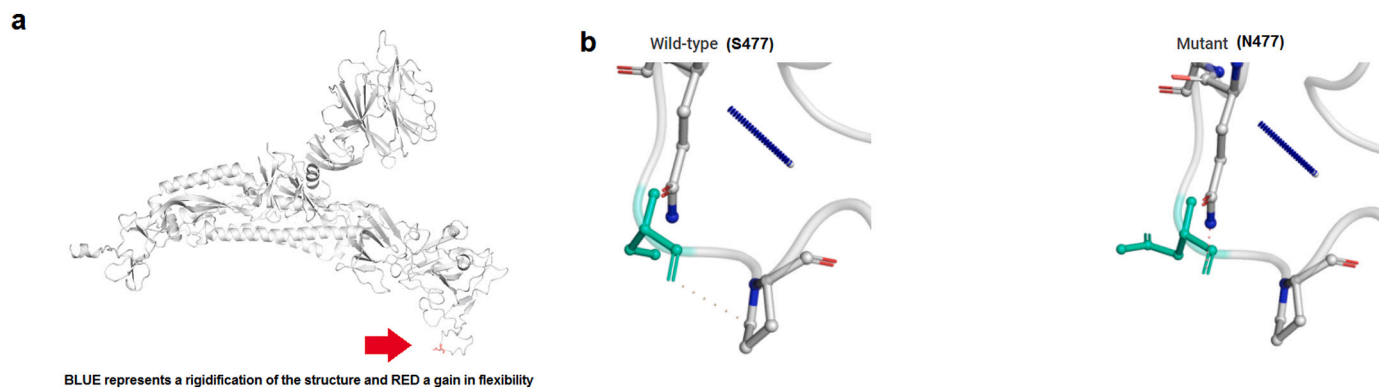
Fig. 11. Evaluated important properties of S477N. (a) Vibrational entropy energy of S477N with a visual representation through ΔΔG score prediction. (b) Interatomic interactions of wild type to mutant type S477N mutation.

model was developed to understand the atomic fluctuations of the 3D space of S-glycoprotein in virtual mode. It displays the 3D landscape (atomic fluctuations) of both the wild and mutant-type S-glycoproteins (Fig. S3B). Moreover, visual analysis of deformation energies was also observed for the 3D space of S-glycoprotein, both in wild and mutant types (Fig. S3C). Luan et al. have calculated ΔΔG for N501Y mutation for sRBD-CB6 (0.62 kcal·mol^{-1}) and sRBD-hACE2 (−0.81 kcal·mol^{-1}) binding [70].

3.5.4. Mapping the properties of Q493K

Like other mutations, we analyzed the ΔΔG of the Q493K mutation, and it was observed as 0.470 kcal/mol (Fig. 9A). Similarly, we found ΔΔG ENCoM to be 0.066 kcal/mol (destabilizing). At the same time, we analyzed ΔΔG mCSM (0.194 kcal/mol, destabilizing), ΔΔG SDM (0.580

kcal/mol, stabilizing), and ΔΔG DUET (0.794 kcal/mol, destabilizing). The Δ vibrational entropy energy between wild and mutant types was observed as ΔΔSVib ENCoM (−0.082 kcal.mol^{-1}.K^{-1}). The result shows a decrease in molecule flexibility. Simultaneously, we found the interatomic interactions of the Q493K mutation for the wild and mutant-type residues along with their adjacent residues involved in the interaction (Fig. 9B). The fluctuation of Q493K in the wild and mutant-type residues was also observed (Fig. S4A). We found that atomic fluctuations indicate a model of the fluctuation in the 3D space of the wild and mutant type S-glycoproteins (Fig. S4B). For mutation (Q493K), the visual analysis of deformation energies was observed in the 3D landscape of both the wild and mutant type S-glycoproteins (Fig. S4C).
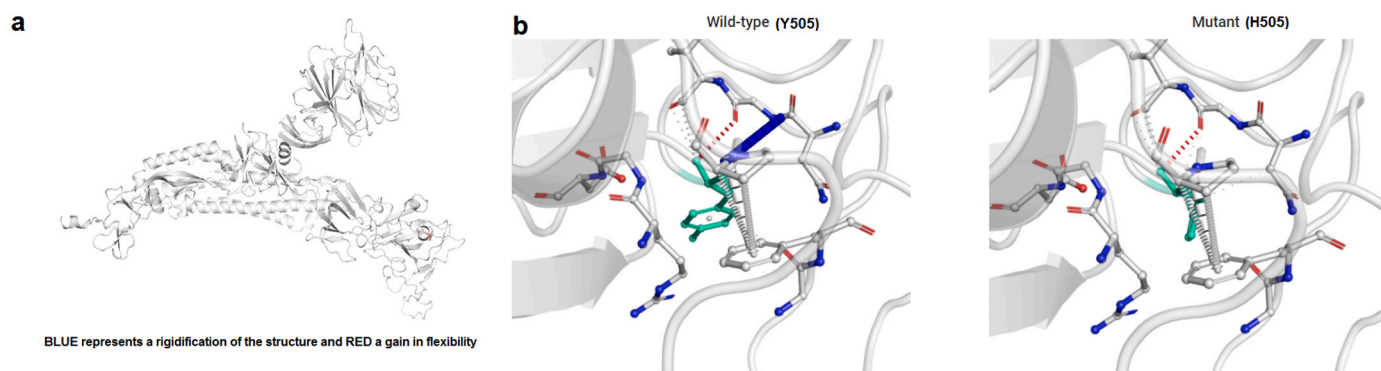
Fig. 12. Mapped noteworthy properties of Y505H. (a) Vibrational entropy energy of Y505H with a visual representation through ΔΔG score prediction. (b) Interatomic interactions of wild type to mutant type Y505H mutation.
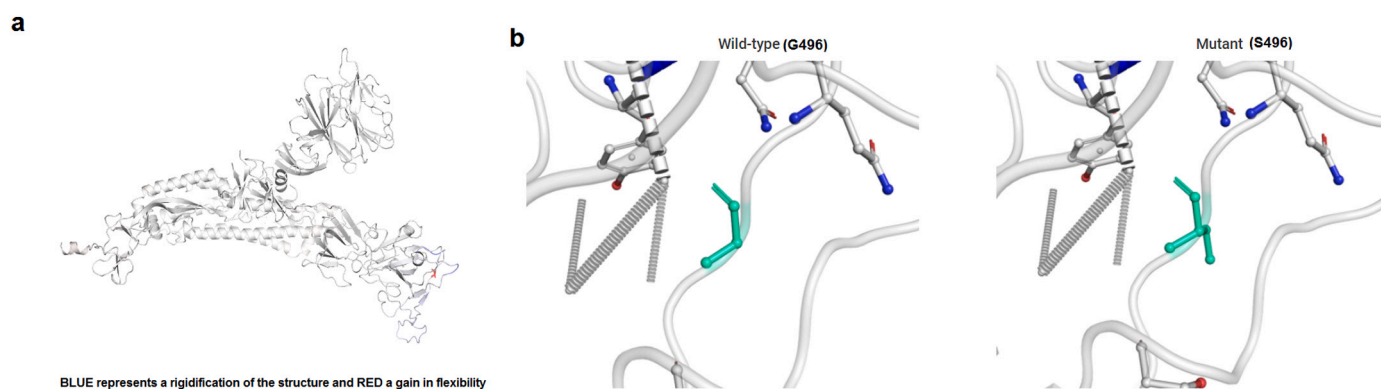
Fig. 13. Illustrated significant properties of G496S. (a) Vibrational entropy energy of G496S with a visual representation through ΔΔG score prediction. (b) Interatomic interactions of wild type to mutant type G496S mutation.

3.5.5. Mapping the properties of K417N

The analysis outcome for K417N mutation are ΔΔG (−0.932 kcal//mol) (Fig. 10A), ΔΔG ENCoM (−0.677 kcal/mol, destabilizing), ΔΔG mCSM (−1.138 kcal/mol; destabilizing), ΔΔG SDM (−0.280 kcal/mol; destabilizing) and ΔΔG DUET (−1.123 kcal/mol; destabilizing). We analyzed Δ vibrational entropy energy between wild and mutant types (ΔΔSVib ENCoM: 0.846 kcal.mol^{-1}.K^{-1}), and an increase in the molecule flexibility of the model was noted. Interatomic interactions provided information about the interactions of residues in both wild and mutant types (Fig. 10B). We also observed the fluctuation of the wild and mutant-type residues of K417N mutation (Fig. S5A). Visual analysis of atomic fluctuations of K417N mutation in S-glycoprotein showed the atomic fluctuations of the 3D space of S-glycoprotein in wild and mutant types (Fig. S5B). At the same time, we performed an analysis to understand the visual analysis of deformation energies. It demonstrated the amount of local flexibility of the 3D space of S-glycoprotein in wild and mutant types (Fig. S5C). Luan et al. have calculated ΔΔG for K417N mutation for sRBD-CB6 (9.59 kcal·mol^{-1}) and sRBD-hACE2 (1.48 kcal·mol^{-1}) binding [71].

3.5.6. Mapping the properties of S477N

The ΔΔG was analyzed to understand the characteristics of S477N mutation, and it was observed to be 0.628 kcal/mol. (Fig. 11A). Again, ΔΔG ENCoM (0.064 kcal/mol, destabilizing), ΔΔG mCSM (−0.215 kcal/mol; destabilizing), ΔΔG SDM (0.780 kcal/mol; stabilizing) and ΔΔG DUET (0.235 kcal/mol; stabilizing) were also evaluated for S477N mutation. Δ vibrational entropy energy between wild and mutant types showed ΔΔSVib ENCoM as −0.080 kcal.mol^{-1}.K^{-1}. A decrease in molecule flexibility of the model was evident from the analysis. Simultaneously, the interatomic interactions were observed (Fig. 11B), and residue and bonds involved in the interaction were recorded. The RMS fluctuation in all residues for S477N mutation of S-glycoprotein was noted for the wild and mutant type residues (Fig. S6A). The fluctuation was observed in the residues, which are more or less similar to other mutations. We observed the atomic fluctuations in the 3D configuration of the S-glycoprotein, demonstrating the atomic fluctuations of both the wild and mutant types (Fig. S6B). Lastly, we analyzed the visual analysis of deformation energies to demonstrate the quantity of local flexibility of the 3D arrangement, both in the wild and mutant type S-glycoproteins (Fig. S6C).

3.5.7. Mapping the properties of Y505H

The ΔΔG estimation outcome of Y505H mutation was −0.510 kcal/mol (Fig. 12A). At the same time, ΔΔG ENCoM (−0.305 kcal/mol, destabilizing) was also analyzed. Similarly, other structure-based analyses showed three parameters i) ΔΔG mCSM as −0.119 kcal/mol, destabilizing; ii) ΔΔG SDM as 0.380 kcal/mol, stabilizing and iii) ΔΔG DUET as 0.143 kcal/mol, stabilizing. The analyzed Δ vibrational entropy energy between wild and mutant types was noted as ΔΔSVib ENCoM (0.381 kcal.mol^{-1}.K^{-1}). Similarly, the interatomic interactions of Y505H were recorded for wild and mutant-type residues (Fig. 12B). The neighboring residues involved in the interaction were also observed. Simultaneously, the fluctuation of both the wild and mutant-type residues was recorded (Fig. S7A). The atomic fluctuations of Y505H mutation in the virtual model and 3D arrangement of the S-glycoprotein for wild and mutant types are depicted in Fig. S7B. Concurrently, the visual analysis of deformation energies of Y505H mutation was observed in the 3D model of S-glycoprotein in both the wild and mutant types (Fig. S7C).

3.5.8. Mapping the properties of G496S

Like other mutations, the ΔΔG evaluation of the G496S mutation was −0.097 kcal/mol (Fig. 13A). The ΔΔG ENCoM (−0.014 kcal/mol,

destabilizing), ΔΔG mCSM (−0.763 kcal/mol kcal/mol, destabilizing), ΔΔG SDM (−1.010 kcal/mol, destabilizing) and ΔΔG DUET (−0.614 kcal/mol, destabilizing) were also recorded. The Δ vibration entropy energy between wild and mutant types was observed as ΔΔSVib ENCoM (0.018 kcal.mol^{-1}.K^{-1}). The result shows an increase in molecule flexibility. Concurrently, the interatomic interactions of the G496S mutation for wild and mutant type residues with their nearby residues involved in the interaction are shown in Fig. 13B. The fluctuation of G496S mutation pointing out the wild and mutant-type residues was also observed (Fig. S8A). The atomic fluctuations indicate a model of the fluctuation in the 3D landscape of the wild and mutant types of S-glycoproteins (Fig. S8B). For mutation (G496S), the visual analysis of deformation energies was observed in the 3D arrangement of the wild and mutant type S-glycoproteins (Fig. S8C).

4. Discussion

Presently, more than 20 countries throughout the globe have confirmed the spread of the Omicron variant. Scientists are continuously trying to understand the characteristics of the Omicron variant, and researchers from Belgium reported that the variant could spread much faster than the Delta variant [72]. Therefore, scientists have raised the alarm for the Omicron variant as a global health concern, and a global health alert has also been issued [73].

The preliminary observation found that the Omicron variant is a heavily mutated variant with several mutations, and we mapped the significant mutations of the variant. The comparative mutations studies inform us of several additional mutations throughout the non-structural and structural proteins of the Omicron (Fig. 1E).

We also found several additional mutations within the S-glycoprotein of the Omicron variant compared to three other VoC, especially in the RBD regions. In RBD, we found one significant mutation (N501Y) in Alpha; three important mutations (K417T, E484K, N501Y) in Gamma; and two significant mutations (L452R, T478K) in Delta. At the same time, we found that the Omicron variant contains 15 critical mutations in the RBD region (Table 2). Moreover, our analysis found no significant mutation in the RBM of Alpha; two significant mutations (E484K, N501Y) in Gamma; and two significant mutations (L452R, T478K) in Delta. Similarly, our analysis showed that the Omicron variant contains ten essential mutations in the RBM region (N440K, G446S, S477N, T478K, E484A, Q493K, G496S, Q498R, N501Y, Y505H).

However, the question is how effective the mutations of Omicron are? In the current scenario, an essential question throughout the world is: are these mutations responsible for antibody escape or vaccine escape? [72]. Some studies have been performed to understand the antibody escape or partial vaccine escape of the emerging variants and noted nAb escape or partial vaccine escape properties [64,74]. Very low protection against the variant while using the neutralizing sera from double vaccinated participants or convalescent sera from boosted individuals was observed [75]. However, mRNA vaccines showed potent neutralization for the Omicron variant [76]. In this direction, we have performed a bioinformatics study to comprehend the mutations in antibody binding regions or the mutations in adjacent antibody binding regions of S-glycoprotein in the Omicron variant and reported several mutations in S-glycoprotein regions (Table 3).

Our study chose eight mutations (D614G, E484A, N501Y, Q493K, K417N, S477N, Y505H, and G496S) of Omicron S-glycoprotein to map the significant virulent properties. Among the eight mutations, seven mutations (E484A, N501Y, Q493K, K417N, S477N, Y505H, and G496S) are located in the RBD region, and one mutation (D614G) outside the RBD region of the S-glycoprotein (Fig. 1b). It has already been reported that mutations in the RBD region of the Omicron have a significant role in augmenting S-glycoprotein's binding affinity to the ACE2 receptor and thus, increasing the infectivity [77]. Furthermore, due to many significant mutations in S-glycoprotein, the Omicron variant is prominent for its antibody escape or antibody-mediated neutralization

Table 4
Major mutations that were chosen for our study and their characteristics reported by different researchers.

Sl. No.	Significant mutations of Omicron variant	Features of mutations	Reference
1.	D614G	Enhance the main protein chain flexibility which shown high infectivity rate with better binding affinity of S-protein to the ACE2 receptor. This mutation boost up the viral fitness to amplify replication and transmission property of SARS-CoV-2 virus.	[85,87,90,91]
2.	E484A	Crucial role in the advancement of viral infectivity, transmissibility, and/or antigenicity. This mutation reduces the neutralization potency of antibodies.	[94,95]
3.	N501Y	Increasing the electrostatic interactions between S-protein and ACE2 by a strong hydrogen bond near the mutation site. Which also affect viral-host cells fusion and increased viral transmission rate.	[1,2,96,97]
4.	Q493K	This mutation considerably contributes to the binding energies of the RBD of S-protein and ACE2 and almost doubled the electrostatic potential S-protein-ACE2 complex.	[98,99]
5.	K417N	The RBD-ACE2 interactions were expressively increased due to K417N mutation by increasing the RBD-ACE2 free energy of binding. This single mutation also destabilizes the stated interaction complex through a combination of slower binding and faster dissociation.	[1,87,97,100]
6.	S477N	This important mutation results in increased binding affinity of S-protein RBD region for the ACE2 receptor. It also facilitates the immune escape mechanism by increasing receptor-binding affinity freely on antibody recognition of epitopes.	[1,101,102]
7.	Y505H	Y505H mutation causing in reduced protein stability and an augmented risk of viral disease	[103]
8.	G496S	It change the shape of the receptor-binding motif (RBM) and generates a steric interference for the binding of Abs to the RBD of S-protein, results in loss of Ab-RBD interactions.	[104,105]

resistance and partial vaccine escape [78–80]. Concurrently, we also reported from our previous bioinformatics study that mutations in the RBD region in Omicron have a significant role in antibody escape [81]. Therefore, we chose seven mutations (E484A, N501Y, Q493K, K417N, S477N, Y505H, and G496S) in the RBD regions out of eight mutations selected for our study. D614G is a significant mutation reported by several scientists for its essential role in augmenting the receptor binding affinity of S-glycoprotein and thus, augmenting the infectivity and re-infectivity [82–84]. D614G is found in most emerging variants, especially all VoC and VoI [85,88]. All these mutations have already been reported from other variants for their significant characteristics and have been found associated with increasing infectivity rate with the better binding affinity of S-glycoprotein to the ACE2 receptor, reduction of the neutralization potency of antibodies, etc. (Table 4). Furthermore, our study has tried to analyze all the eight mutations to understand the stabilizing or destabilizing properties and evaluate S-glycoprotein's

Table 5
Comparative analysis of or ΔΔG score of significant mutations of Omicron variant.

Sl no.	Significant mutations of Omicron variant	ΔΔG Prediction	NMA based prediction	Other structure-based predictions			Δ Vibrational entropy energy between wild-type and mutant	Remark
		ΔΔG (kcal/mol)	ΔΔG ENCoM (kcal/mol)	ΔΔG mCSM (kcal/mol)	ΔΔG SDM (kcal/mol)	ΔΔG DUET (kcal/mol)	ΔΔS$_{Vib}$ ENCoM (kcal.mol^{-1}.K^{-1})	
1	D614G	0.351, Stabilizing	−0.134, Destabilizing	−0.514, Destabilizing	2.510, Stabilizing	0.171, Stabilizing	0.168	Increase of molecular flexibility
2	E484A	−0.456, Destabilizing	−0.377, Destabilizing	−0.415, Destabilizing	0.320, Stabilizing	−0.128, Destabilizing	0.471	Increase of molecular flexibility
3	N501Y	−0.203, Destabilizing	−0.094, Destabilizing	−0.457, Destabilizing	0.280, Stabilizing	−0.471, Destabilizing	0.117	Increase of molecular flexibility
4	Q493K	0.470, Stabilizing	0.066, Destabilizing	0.194, Stabilizing	0.580, Stabilizing	0.794, Stabilizing	−0.082	Decrease of molecular flexibility
5	K417N	−0.932, Destabilizing	−0.677, Destabilizing	−1.138, Destabilizing	−0.280, Destabilizing	−1.123, Destabilizing	0.846	Increase of molecular flexibility
6	S477N	0.628, Stabilizing	0.064, Destabilizing	−0.215, Destabilizing	0.780, Stabilizing	0.235, Stabilizing	−0.080	Decrease of molecular flexibility
7	Y505H	−0.510, Destabilizing	−0.305, Destabilizing	−0.119, Destabilizing	0.380, Stabilizing	0.143, Stabilizing	0.381	Increase of molecular flexibility
8	G496S	−0.097, Destabilizing	−0.014, Destabilizing	−0.763, Destabilizing	−1.010, Destabilizing	−0.614, Destabilizing	0.018	Increase of molecular flexibility
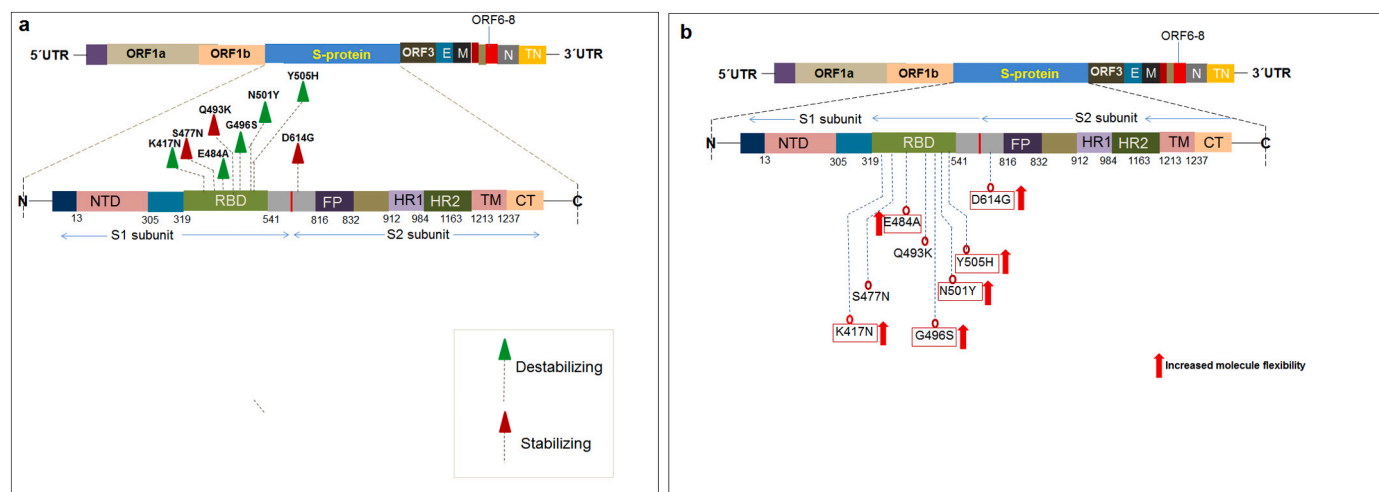
Fig. 14. Schematic representation shows Omicron S-glycoprotein significant mutations, and their effects on stability and flexibility changes due to amino acid substitution (a) Schematic representation shows significant mutations of Omicron S-glycoprotein and their effects on stability. (b) Schematic representation shows significant mutations of Omicron S-glycoprotein and their effects on flexibility.

increased or decreased molecule flexibility. These altered properties can help S-glycoprotein interact with the ACE2 receptor differently. Therefore, our analyses will help characterize the mutations of the S-glycoprotein of Omicron and the properties concerning these mutations.

Finally, the study tried to characterize the significant properties of D614G, E484A, N501Y, Q493K, K417N, S477N, Y505H, and G496S of the Omicron variant. In that direction, we have chosen the significant mutations that are located in RBD, one from RBM, and the mutations in nAb binding regions. We have also considered the mutations which have a role in the immune escape, infectivity or re-infectivity, or vaccine escape. Previously, it has been reported that D614G mutation has a role in the immune escape, infectivity, or re-infectivity [9,18]. Scientists have already reported that the E484K mutation has the property of antibody evasion [1,87]. Therefore, we have chosen all these mutations

for characterization. Several scientists have analyzed ΔΔG score for significant mutations of other SARS-CoV-2 variants such as Delta, Lambda, and Kappa [88]. Here we analyzed the ΔΔG score of Omicron to understand the effects of mutation on molecular flexibility, interatomic interactions between the residues of wild and mutant types, atomic fluctuations, and deformation energies residues in wild and mutant type residues. We also performed a comparative analysis of ΔΔG score of significant mutations (Table 5). The ΔΔG score study outcome shows that D614G, Q493K, and S477N mutations stabilize with 0.351 kcal/mol, 0.470 kcal/mol, and 0.628 kcal/mol, respectively. Other mutations showed destabilizing results. On the other hand, our study noted that the D614G, E484A, N501Y, K417N, Y505H, and G496S mutation augmented the molecule flexibility of S-glycoprotein. However, our evaluated atomic fluctuations and deformation energies of all

mutations (D614G, E484A, N501Y, Q493K, K417N, S477N, Y505H, G496S) have shown a similar kind of result for all of these mutations (Fig. S1 to Fig. S8).

Previously, researchers have categorized several SARS-CoV-2 mutations concerning stabilizing and destabilizing properties. They have used the COVID-3D server to analyze the stabilizing/destabilizing properties of the mutation of SARS-CoV-2 variants [89]. DynaMut is a widely used server that can evaluate mutations' stabilizing and destabilizing properties and analyze a protein's increased or decreased molecular flexibility [53]. Benvenuto et al. have analyzed three mutations of the SARS-CoV-2 genome, which was collected from Italian patients. These mutations were characterized using the DynaMut server [90]. Another study characterized the L452R, E484Q, and P681R mutations of the Indian variant (B.1.617) and calculated ΔΔG score to understand the protein stability using the DynaMut server [91]. In all of these cases, the researchers did not evaluate the MD simulation to check the flexibility of S-glycoprotein and analyze the increased/decreased molecular flexibility of S-glycoprotein to interact with the human ACE2 receptor using DynaMut. However, our study utilized the DynaMut server to analyze S-glycoprotein's increased/decreased molecular flexibility to interact with the ACE2 receptor and stabilizing /destabilizing properties of eight mutations of the Omicron variant (Fig. 14). In this respect, our study has illustrated the properties of eight mutations of the Omicron variant very rapidly, which might be very significant for future researchers from the pandemic point of view.

Our analyzed mutations are located in two significant regions of the S-glycoprotein. The seven mutations (E484A, N501Y, Q493K, K417N, S477N, Y505H, G496S) are located in the Omicron RBD. Two mutations (S477N and D614G) were observed in the possible epitopic regions. The stabilizing mutation might affect the structure of the Omicron spike (S). It has been noted that stabilizing mutation assists to augment in the rigidity of the structure of S-protein. The improved rigidities of the Omicron spike structure may provide a stable conformation to the Omicron spike. The stable conformation of the spike may ultimately influence the binding interface of the Omicron spike to the ACE2 receptor [81,82]. Finally, it has been noted that stabilizing mutation and destabilizing mutations properties of the Omicron's spike structure help balance these two mutations' properties (stabilizing mutation and destabilizing), which leads to an effectively- maintained structure of the protein [82].

5. Limitations

The Omicron variant has made the pandemic critical due to its high infection properties and antibody escape characteristics [79–83]. Our study evaluated eight mutations of the Omicron variant and their increased/decreased molecular flexibility of S-glycoprotein to interact with the ACE2 receptor using DynaMut in a short frame of time. It may be a limitation of our study. However, this rapidly generated data may be very helpful from a pandemic point of view and when Omicron is a VoC. Our analyzed data will help researchers working with the Omicron variant. However, we urge future researchers to understand more about the changes in the flexibility of S-glycoprotein due to mutations. Finally, the understanding will help to explain how the flexibility changes affect the interaction property of S-glycoprotein during the interaction with the ACE2 receptor.

Moreover, in this study, we have used the DynaMut server to analyze stabilizing/destabilizing properties of eight mutations of the Omicron variant and calculated the ΔΔGscore. Other researchers have noted a similar kind to ΔΔG scores during the characterization of the mutations of SARS-CoV-2 variants using the same server [92]. More studies are needed in this direction to confirm our findings.

Meanwhile, our data from rapid bioinformatics need further validation with the experimental work. More research is required to understand deeper insight into the flexibility of the spike protein with the stronger or weak binding to either ACE2 receptor or nAbs. We have not validated our data through experimental work, which is another

limitation of our study. We also urge future researchers to study the association between receptor or antibody binding to provide much evidence into the flexibility of the spike protein and its interaction with either ACE2 receptor or nAbs.

6. Conclusion

The present study represents a snapshot of the mutation pattern of Omicron, considering all structural proteins and non-structural proteins. We also tried to capture the mutation pattern of S-glycoprotein. Our statistical model of mutation analysis shows S-glycoprotein of Omicron having the highest mutations compared the all structural proteins (E, M, N) and non-structural proteins (nsp3, nsp4, nsp5, nsp6, nsp12, nsp14) of Omicron (Fig. 2B). Moreover, the statistical model revealed that RBD has the highest number of mutations compared to all other regions of S-glycoprotein (Fig. 2D). From this model, our study also noted the second-highest number of mutations in the NTD region of S-glycoprotein (Fig. 2D). Our previous study observed that mutations in RBD and NTD have a significant role in antibody escape [83]. Therefore, due to the significant number of mutations in RBD and NTD, the Omicron variant might possess a prominent nAb escape property. We also observed the effects of missense mutations on the thermodynamic stability of S-glycoprotein through the ΔΔG score prediction (the change in Gibbs Free Energy). It was found that among RBD mutations, two mutations (Q493K and S477N) were stabilizing. Therefore, these two mutations might help the structural stability of RBD of S-glycoprotein of Omicron and contribute to the interaction property like receptor binding. These properties might finally confer the antibody escape and augment receptor binding property. Our analysis also found that D614G is a stabilizing mutation. Previously it has been observed that D614G helps in increased receptor binding, which augments the infectivity and re-infectivity [84–86,93]. Stabilized property of D614G might also help stable receptor binding property to S-glycoprotein to provide the infectivity property to Omicron. Finally, our analysis found that D614G, E484A, N501Y, K417N, Y505H, and G496S mutations increased the molecule flexibility of S-glycoprotein to interact with the ACE2 receptor, which might increase Omicron variant infectivity.

Presently, the burning question is whether our immunity can defend against the newly developing variants or whether the available vaccines can fight against these variants? Several other questions are raised throughout the world after the appearance of the Omicron variant. Some questions are i) how fast can the variant spread? ii) can every country tackle the variant? ii) what are the primary mutations with immune or antibody escape properties? Future researchers might generate a pseudovirus particle with primary mutations to answer these questions. In this direction, our study (mutation pattern of Omicron, stabilizing/destabilizing properties, and increased/decreased molecular flexibility of S-glycoprotein due to mutation) will benefit future researchers in choosing the proper mutations for future experiments.

Supplementary data to this article can be found online at https://doi.org/10.1016/j.ijbiomac.2022.07.254.

Abbreviations

VoC	Variant of concern
VoI	Variant of interest
RBD	Receptor binding domain
RBM	Receptor binding motif
ACE2	Angiotensin-Converting Enzyme 2
nAb	neutralizing antibody
WHO	World Health Organization
NTD	N-terminal domain
nsp	non-structural protein
S-protein	Spike protein
NMA	Normal Mode Analysis
SDM	Site Directed Mutator

Vib ENCoM   Vibrational Entropy energy
Δ   Delta
RMSF   Root Mean Square Fluctuation
MATLAB   MATrix LABoratory
ENCoM   Elastic Network Contact Model
mCSM   mutation Cutoff Scanning Matrix
ΔΔSVib   vibrational entropy energy

CRediT authorship contribution statement

CC contributed to the conception, design, data collection, and analysis of the study. The first draft of the manuscript was written by CC. MB performed the data validation. ARS validated data, reviewed and edited the manuscript. BM performed the data validation. All authors read and approved the final manuscript.

Availability of data and material

The datasets generated during and/or analyzed during the current study are available within the submitted manuscript.

Declaration of competing interest

The authors declare no competing interest.

References

[1] C. Chakraborty, M. Bhattacharya, A.R. Sharma, Present variants of concern and variants of interest of severe acute respiratory syndrome coronavirus 2: their significant mutations in S-glycoprotein, infectivity, re-infectivity, immune escape and vaccines activity, Rev. Med. Virol. 32 (2021) 1–14, e2270.

[2] C. Chakraborty, A.R. Sharma, M. Bhattacharya, G. Agoramoorthy, S.-S. Lee, Evolution, mode of transmission, and mutational landscape of newly emerging SARS-CoV-2 variants, MBio 12 (4) (2021), e01140-21.

[3] A. Aleem, A.S. AB, A.K. Slenker, Emerging variants of SARS-CoV-2 and novel therapeutics against coronavirus (COVID-19), in: StatPearls [Internet] 2, StatPearls Publishing, Treasure Island (FL), 2021.

[4] D. Mercatelli, F.M. Giorgi, Geographic and genomic distribution of SARS-CoV-2 mutations, Front. Microbiol. 11 (2020) 1800.

[5] A.E. Castillo, B. Parra, P. Tapia, J. Lagos, L. Arata, A. Acevedo, W. Andrade, G. Leal, C. Tambley, P. Bustos, Geographical distribution of genetic variants and lineages of SARS-CoV-2 in Chile, Front. Public Health 8 (2020) 525.

[6] M.F. Boni, P. Lemey, X. Jiang, T.T.-Y. Lam, B.W. Perry, T.A. Castoe, A. Rambaut, D.L. Robertson, Evolutionary origins of the SARS-CoV-2 sarbecovirus lineage responsible for the COVID-19 pandemic, Nat. Microbiol. 5 (11) (2020) 1408–1417.

[7] M. Goyal, K. De Bruyne, A. van Belkum, B. West, Different SARS-CoV-2 haplotypes associate with geographic origin and case fatality rates of COVID-19 patients, Infect. Genet. Evol. 90 (2021), 104730.

[8] S. Duffy, Why are RNA virus mutation rates so damn high? PLoS Biol. 16 (8) (2018), e3000003.

[9] C. Chakraborty, A. Saha, A.R. Sharma, M. Bhattacharya, S.-S. Lee, G. Agoramoorthy, D614G mutation eventuates in all VOI and VOC in SARS-CoV-2: is it part of the positive selection pioneered by Darwin? Mol.Ther.Nucleic Acids 26 (2021) 237–241.

[10] C. Chakraborty, A.R. Sharma, M. Bhattacharya, G. Agoramoorthy, S.-S. Lee, A paradigm shift in the combination changes of SARS-CoV-2 variants and increased spread of Delta variant (B.1.617.2) across the world, Aging Dis. 13 (2021) 927–942. https://doi.org/10.14336/AD.2021.1117.

[11] WHO, Update on Omicron. https://www.who.int/news/item/28-11-2021-update-on-omicron, 2021.

[12] X. Ou, Y. Liu, X. Lei, P. Li, D. Mi, L. Ren, L. Guo, R. Guo, T. Chen, J. Hu, Characterization of spike glycoprotein of SARS-CoV-2 on virus entry and its immune cross-reactivity with SARS-CoV, Nat. Commun. 11 (1) (2020) 1–12.

[13] C. Chakraborty, A. Sharma, B. Mallick, M. Bhattacharya, G. Sharma, S. Lee, Evaluation of molecular interaction, physicochemical parameters and conserved pattern of SARS-CoV-2 spike RBD and hACE2: in silico and molecular dynamics approach, Eur. Rev. Med. Pharmacol. Sci. 25 (3) (2021) 1708–1723.

[14] L. Duan, Q. Zheng, H. Zhang, Y. Niu, Y. Lou, H. Wang, The SARS-CoV-2 spike glycoprotein biosynthesis, structure, function, and antigenicity: implications for the design of spike-based vaccine immunogens, Front. Immunol. 11 (2020) 2593.

[15] L. Dai, G.F. Gao, Viral targets for vaccines against COVID-19, Nat. Rev. Immunol. 21 (2) (2021) 73–82.

[16] A.C. Walls, Y.J. Park, M.A. Tortorici, A. Wall, A.T. McGuire, D. Veesler, Structure, function, and antigenicity of the SARS-CoV-2 spike glycoprotein, Cell 181 (2020) 281–292.

[17] M. Singh, V. Bansal, C. Feschotte, A single-cell RNA expression map of human coronavirus entry factors, Cell Rep. 32 (2020), 108175.

[18] I. Mercurio, V. Tragni, F. Busto, A. De Grassi, C.L. Pierri, Protein structure analysis of the interactions between SARS-CoV-2 spike protein and the human ACE2 receptor: from conformational changes to novel neutralizing antibodies, Cell. Mol. Life Sci. 78 (2021) 1501–1522.

[19] D. Wrapp, N. Wang, K.S. Corbett, J.A. Goldsmith, C.L. Hsieh, O. Abiona, et al., Cryo-EM structure of the 2019-nCoV spike in the prefusion conformation, Science 367 (6483) (2020) 1260–1263.

[20] V. Tragni, F. Preziusi, L. Laera, A. Onofrio, I. Mercurio, S. Todisco, et al., Modeling SARS-CoV-2 spike/ACE2 protein–protein interactions for predicting the binding affinity of new spike variants for ACE2, and novel ACE2 structurally related human protein targets, for COVID-19 handling in the 3PM context, EPMA J. (2022) 1–27.

[21] R. Sasisekharan, Preparing for the future—nanobodies for Covid-19? N. Engl. J. Med. 384 (16) (2021) 1568–1571.

[22] J. Huo, J. Mikolajek, A. Le Bas, J.J. Clark, P. Sharma, A. Kipar, et al., A potent SARS-CoV-2 neutralising nanobody shows therapeutic efficacy in the Syrian golden hamster model of COVID-19, Nat. Commun. 12 (1) (2021) 1–18.

[23] B. Turoňová, M. Sikora, C. Schürmann, W.J. Hagen, S. Welsch, F.E. Blanc, et al., In situ structural analysis of SARS-CoV-2 spike reveals flexibility mediated by three hinges, Science 370 (6513) (2020) 203–208.

[24] C.L. Pierri, SARS-CoV-2 spike protein: flexibility as a new target for fighting infection, Signal Transduct. Target. Ther. 5 (1) (2020) 1–3.

[25] W.T. Harvey, A.M. Carabelli, B. Jackson, R.K. Gupta, E.C. Thomson, E.M. Harrison, C. Ludden, R. Reeve, A. Rambaut, S.J. Peacock, SARS-CoV-2 variants, spike mutations and immune escape, Nat. Rev. Microbiol. 19 (7) (2021) 409–424.

[26] S. Teng, A. Sobitan, R. Rhoades, D. Liu, Q. Tang, Systemic effects of missense mutations on SARS-CoV-2 spike glycoprotein stability and receptor-binding affinity, Brief. Bioinform. 22 (2) (2021) 1239–1253.

[27] M. Bhattacharya, S. Chatterjee, A.R. Sharma, G. Agoramoorthy, C. Chakraborty, D614G mutation and SARS-CoV-2: impact on S-protein structure, function, infectivity, and immunity, Appl. Microbiol. Biotechnol. (2021) 1–11.

[28] K.O. Saunders, E. Lee, R. Parks, D.R. Martinez, D. Li, H. Chen, R.J. Edwards, S. Gobeil, M. Barr, K. Mansouri, Neutralizing antibody vaccine for pandemic and pre-emergent coronaviruses, Nature (2021) 1–7.

[29] Y. Weisblum, F. Schmidt, F. Zhang, J. DaSilva, D. Poston, J.C. Lorenzi, F. Muecksch, M. Rutkowska, H.-H. Hoffmann, E. Michailidis, Escape from neutralizing antibodies by SARS-CoV-2 spike protein variants, elife 9 (2020), e61312.

[30] A.J. Greaney, T.N. Starr, P. Gilchuk, S.J. Zost, E. Binshtein, A.N. Loes, S.K. Hilton, J. Huddleston, R. Eguia, K.H. Crawford, Complete mapping of mutations to the SARS-CoV-2 Spike receptor-binding domain that escape antibody recognition, Cell Host Microbe 29 (1) (2021) 44–57, e9.

[31] C. Chakraborty, M. Bhattacharya, A.R. Sharma, Emerging mutations in the SARS-CoV-2 variants and their role in antibody escape to small molecule-based therapeutic resistance, Curr. Opin. Pharmacol. 62 (2021) 64–73.

[32] W. Dejnirattisai, J. Huo, D. Zhou, J. Zahradník, P. Supasa, C. Liu, H.M. Duyvesteyn, H.M. Ginn, A.J. Mentzer, A. Tuekprakhon, SARS-CoV-2 Omicron-B. 1.1. 529 leads to widespread escape from neutralizing antibody responses, Cell 185 (2022) 467–484.e15.

[33] Y. Cao, J. Wang, F. Jian, T. Xiao, W. Song, A. Yisimayi, W. Huang, Q. Li, P. Wang, R. An, Omicron escapes the majority of existing SARS-CoV-2 neutralizing antibodies, Nature (2021) 1–9.

[34] E. Cameroni, J.E. Bowen, L.E. Rosen, C. Saliba, S.K. Zepeda, K. Culap, D. Pinto, L.A. VanBlargan, A.De Marco, J. di Iulio, Broadly neutralizing antibodies overcome SARS-CoV-2 Omicron antigenic shift, Nature (2021) 1–9.

[35] D. Planas, N. Saunders, P. Maes, F. Guivel-Benhassine, C. Planchais, J. Buchrieser, W.-H. Bolland, F. Porrot, I. Staropoli, F. Lemoine, Considerable escape of SARS-CoV-2 Omicron to antibody neutralization, Nature (2021) 1–7.

[36] D. Planas, D. Veyer, A. Baidaliuk, I. Staropoli, F. Guivel-Benhassine, M.M. Rajah, C. Planchais, F. Porrot, N. Robillard, J. Puech, Reduced sensitivity of SARS-CoV-2 variant Delta to antibody neutralization, Nature 596 (7871) (2021) 276–280.

[37] C. Davis, N. Logan, G. Tyson, R. Orton, W.T. Harvey, J.S. Perkins, G. Mollett, R.M. Blacow, , C.-G.U. Consortium, T.P. Peacock, Reduced neutralisation of the Delta (B. 1.617. 2) SARS-CoV-2 variant of concern following vaccination, PLoS Pathog. 17 (12) (2021), e1010022.

[38] L. Bian, Q. Gao, F. Gao, Q. Wang, Q. He, X. Wu, Q. Mao, M. Xu, Z. Liang, Impact of the Delta variant on vaccine efficacy and response strategies, Expert Rev.Vaccines 20 (10) (2021) 1201–1209.

[39] B. Thoma, T.M. Chan, Using Google Scholar to track the scholarly output of research groups, Perspect.Med.Educ. 8 (3) (2019) 201–205.

[40] X. Zuo, Y. Chen, L. Ohno-Machado, H. Xu, How do we share data in COVID-19 research? A systematic review of COVID-19 datasets in PubMed Central Articles, Brief. Bioinform. 22 (2) (2021) 800–811.

[41] J. Chan, S. Oo, C.Y.T. Chor, D. Yim, J.S.K. Chan, A. Harky, COVID-19 and literature evidence: should we publish anything and everything? Acta Bio Medica: Atenei Parmensis 91 (3) (2020), e2020020.

[42] R.K. Farooq, S.U. Rehman, M. Ashiq, N. Siddique, S. Ahmad, Bibliometric analysis of coronavirus disease (COVID-19) literature published in web of science 2019–2020, J. Fam. Community Med. 28 (1) (2021) 1.

[43] CDC, Omicron variant: what you need to know. https://www.cdc.gov/coronavirus/2019-ncov/variants/omicron-variant.html, 2021 (Accessed on 7/12/2021).

[44] CDC, Science Brief: Omicron (B.1.1.529) Variant. https://www.cdc.gov/coronavirus/2019-ncov/science/science-briefs/scientific-brief-omicron-variant.html, 2021 (Accessed on 7/12/2021).

[45] ECDC, Implications of the Further Emergence and Spread of the SARS-CoV-2 B.1.1.529 Variant of Concern (Omicron) for the EU/EEA – First Update, Stockholm, 2021 (Accessed on 7/12/2021).

[46] WHO, Update on Omicron. https://www.who.int/news/item/28-11-2021-update-on-omicron, 2021 (Accessed on 7/12/2021).

[47] Y. Shu, J. McCauley, GISAID: global initiative on sharing all influenza data–from vision to reality, Eurosurveillance 22 (13) (2017) 30494.

[48] S. Elbe, G. Buckland-Merrett, Data, disease and diplomacy: GISAID's innovative contribution to global health, Global Chall. 1 (1) (2017) 33–46.

[49] E. Mathieu, H. Ritchie, E. Ortiz-Ospina, M. Roser, J. Hasell, C. Appel, C. Giattino, L. Rodés-Guirao, A global database of COVID-19 vaccinations, Nat. Hum. Behav. (2021) 1–7.

[50] Nextstrain, Nextstrain SARS-CoV-2 Resources on Nextstrain, 2021 (Accessed on 7/12/2021).

[51] J. Westbrook, Z. Feng, S. Jain, T.N. Bhat, N. Thanki, V. Ravichandran, G.L. Gilliland, W. Bluhm, H. Weissig, D.S. Greer, The protein data bank: unifying the archive, Nucleic Acids Res. 30 (1) (2002) 245–248.

[52] R.A. Laskowski, J.M. Thornton, PDBsum extras: SARS-CoV-2 and AlphaFold models, Protein Sci. 31 (1) (2021) 283–289.

[53] C.H. Rodrigues, D.E. Pires, D.B. Ascher, DynaMut: predicting the impact of mutations on protein conformation, flexibility and stability, Nucleic Acids Res. 46 (W1) (2018) W350–W355.

[54] E. Capriotti, P. Fariselli, I. Rossi, R.A. Casadio, A three-state prediction of single point mutations on protein stability changes, BMC Bioinformatics 9 (2) (2008) 1–9.

[55] V. Frappier, R.J. Najmanovich, A coarse-grained elastic network atom contact model and its use in the simulation of protein dynamics and the prediction of the effect of mutations, PLoS Comput. Biol. 10 (4) (2014), e1003569.

[56] D.E. Pires, D.B. Ascher, T.L. Blundell, mCSM: predicting the effects of mutations in proteins using graph-based signatures, Bioinformatics 30 (3) (2014) 335–342.

[57] A.P. Pandurangan, B. Ochoa-Montaño, D.B. Ascher, T.L. Blundell, SDM: a server for predicting effects of mutations on protein stability, Nucleic Acids Res. 45 (W1) (2017) W229–W235.

[58] D.E. Pires, D.B. Ascher, T.L. Blundell, DUET: a server for predicting effects of mutations on protein stability using an integrated computational approach, Nucleic Acids Res. 42 (W1) (2014) W314–W319.

[59] M. Goethe, I. Fita, J.M. Rubi, Vibrational entropy of a protein: large differences between distinct conformations, J. Chem. Theory Comput. 11 (1) (2015) 351–359.

[60] Ø. Hammer, D.A. Harper, P.D. Ryan, PAST: paleontological statistics software package for education and data analysis, Palaeontol. Electron. 4 (1) (2001) 9.

[61] I. MathWorks, MATLAB, High-performance Numeric Computation and Visualization Software: User's Guide: for UNIX Workstations, MathWorks, 1992 (Accessed on 7/12/2021).

[62] L. Scott, N.Y. Hsiao, S. Moyo, L. Singh, H. Tegally, G. Dor, P. Maes, O.G. Pybus, M.U. Kraemer, E. Semenova, S. Bhatt, Track Omicron's spread with molecular data, Science 374 (6574) (2021) 1454–1455, 17.

[63] L. Liu, S. Iketani, Y. Guo, J.F. Chan, M. Wang, L. Liu, Y. Luo, H. Chu, Y. Huang, M.S. Nair, Striking antibody evasion manifested by the Omicron variant of SARS-CoV-2, Nature (2021) 1–8.

[64] M. Hoffmann, N. Krüger, S. Schulz, A. Cossmann, C. Rocha, A. Kempf, I. Nehlmeier, L. Graichen, A.-S. Moldenhauer, M.S. Winkler, The omicron variant is highly resistant against antibody-mediated neutralization–implications for control of the COVID-19 pandemic, Cell 185 (3) (2021) 447–456.e11.

[65] C.O. Barnes, C.A. Jette, M.E. Abernathy, K.M.A. Dam, S.R. Esswein, H.B. Gristick, et al., SARS-CoV-2 neutralizing antibody structures inform therapeutic strategies, Nature 588 (7839) (2020) 682–687.

[66] A.J. Greaney, T.N. Starr, C.O. Barnes, Y. Weisblum, F. Schmidt, M. Caskey, et al., Mapping mutations to the SARS-CoV-2 RBD that escape binding by different classes of antibodies, Nat. Commun. 12 (1) (2021) 1–14.

[67] E. Capriotti, P. Fariselli, I. Rossi, R. Casadio, A three-state prediction of single point mutations on protein stability changes, BMC Bioinformatics 9 (2) (2008) 1–9.

[68] S.C. Vedithi, C.H. Rodrigues, S. Portelli, M.J. Skwark, M. Das, D.B. Ascher, T.L. Blundell, S. Malhotra, Computational saturation mutagenesis to predict structural consequences of systematic mutations in the beta subunit of RNA polymerase in Mycobacterium leprae, Comput.Struct.Biotechnol.J. 18 (2020) 271–286.

[69] H. Wako, S. Endo, Normal mode analysis as a method to derive protein dynamics information from the protein data bank, Biophys. Rev. 9 (6) (2017) 877–893.

[70] B. Luan, H. Wang, T. Huynh, Enhanced binding of the N501Y-mutated SARS-CoV-2 spike protein to the human ACE2 receptor: insights from molecular dynamics simulations, FEBS Lett. 595 (10) (2021) 1454–1461.

[71] B. Luan, T. Huynh, Insights into SARS-CoV-2's mutations for evading human antibodies: sacrifice and survival, J. Med. Chem. (2021), https://doi.org/10.1021/acs.jmedchem.1c00311.

[72] E. Callaway, H. Ledford, How bad is Omicron? What scientists know so far, Nature 600 (7888) (2021) 197–199.

[73] S.J. Gao, H. Guo, G. Luo, Omicron variant (B.1.1.529) of SARS-CoV-2, a global urgent public health alert!, J. Medical Virology 94 (4) (2021) 1255–1256.

[74] S. Cele, L. Jackson, D.S. Khoury, K. Khan, T. Moyo-Gwete, H. Tegally, J.E. San, D. Cromer, C. Scheepers, D.G. Amoako, Omicron extensively but incompletely escapes Pfizer BNT162b2 neutralization, Nature (2021) 1–5.

[75] J.M. Carreño, H. Alshammary, J. Tcheou, G. Singh, A. Raskin, H. Kawabata, L. Sominsky, J. Clark, D.C. Adelsberg, D. Bielak, Activity of convalescent and vaccine serum against SARS-CoV-2 Omicron, Nature 602 (7898) (2021) 682–688.

[76] W.F. Garcia-Beltran, K.J.S. Denis, A. Hoelzemer, E.C. Lam, A.D. Nitido, M.L. Sheehan, C. Berrios, O. Ofoman, C.C. Chang, B.M. Hauser, mRNA-based COVID-19 vaccine boosters induce neutralizing immunity against SARS-CoV-2 Omicron variant, Cell 185 (3) (2022) 457–466.e4.

[77] C.S. Lupala, Y. Ye, H. Chen, X.D. Su, H. Liu, Mutations on RBD of SARS-CoV-2 Omicron variant result in stronger binding to human ACE2 receptor, Biochem. Biophys. Res. Commun. 590 (2022) 34–41.

[78] M. Hoffmann, N. Krüger, S. Schulz, A. Cossmann, C. Rocha, A. Kempf, et al., The omicron variant is highly resistant against antibody-mediated neutralization: implications for control of the COVID-19 pandemic, Cell 185 (3) (2022) 447–456.

[79] C. Chakraborty, A.R. Sharma, M. Bhattacharya, S.S. Lee, A detailed overview of immune escape, antibody escape, partial vaccine escape of SARS-CoV-2 and their emerging variants with escape mutations, Frontiers in Immunology 13 (2020) 801522.

[80] R.K. Mohapatra, R. Tiwari, A.K. Sarangi, M.R. Islam, C. Chakraborty, K. Dhama, Omicron (B.1.1.529) variant of SARS-CoV-2: concerns, challenges, and recent updates, J. Med. Virology (2022), https://doi.org/10.1002/jmv.27633.

[81] J. Ou, Z. Zhou, R. Dai, J. Zhang, S. Zhao, X. Wu, W. Lan, Y. Ren, L. Cui, Q. Lan, L. Lu, V367F mutation in SARS-CoV-2 spike RBD emerging during the early transmission phase enhances viral infectivity through increased human ACE2 receptor binding affinity, J. Virol. 95 (16) (2021), e00617-21.

[82] J.J. Jacob, K. Vasudevan, A.K. Pragasam, K. Gunasekaran, B. Veeraraghavan, A. Mutreja, Evolutionary tracking of SARS-CoV-2 genetic variants highlights an intricate balance of stabilizing and destabilizing mutations, MBio 12 (4) (2020), e01188-21.

[83] M. Bhattacharya, A.R. Sharma, K. Dhama, G. Agoramoorthy, C. Chakraborty, Omicron variant (B.1.1.529) of SARS-CoV-2: understanding mutations in the genome, S-glycoprotein, and antibody-binding regions, GeroScience (2022) 1–19.

[84] L. Zhang, C.B. Jackson, H. Mou, A. Ojha, H. Peng, B.D. Quinlan, et al., SARS-CoV-2 spike-protein D614G mutation increases virion spike density and infectivity, Nat. Commun. 11 (1) (2020) 1–9.

[85] B. Korber, W.M. Fischer, S. Gnanakaran, H. Yoon, J. Theiler, W. Abfalterer, et al., Tracking changes in SARS-CoV-2 spike: evidence that D614G increases infectivity of the COVID-19 virus, Cell 182 (4) (2020) 812–827.

[86] M. Bhattacharya, S. Chatterjee, A.R. Sharma, G. Agoramoorthy, C. Chakraborty, D614G mutation and SARS-CoV-2: impact on S-protein structure, function, infectivity, and immunity, Appl. Microbiol. Biotechnol. 105 (24) (2021) 9035–9045.

[87] C. Chakraborty, A. Saha, A.R. Sharma, M. Bhattacharya, S.S. Lee, G. Agoramoorthy, D614G mutation eventuates in all VOI and VOCin SARS-CoV-2: is it part of the positive selection pioneered by Darwin? Mol.Ther.-Nucleic Acids 26 (2021) 237–241.

[88] C. Chakraborty, A. Saha, A.R. Sharma, M. Bhattacharya, G. Agoramoorthy, S.S. Lee, Evolution, mode of transmission, and mutational landscape of newly emerging SARS-CoV-2 variants, MBio 12 (4) (2021), e01140-21.

[89] B. Lam, Y.J. Kung, J. Lin, S.-H. Tseng, Y.C. Tsai, L. He, G. Castiglione, E. Egbert, E.J. Duh, E.M. Bloch, In vivo characterization of emerging SARS-CoV-2 variant infectivity and human antibody escape potential, Cell Reports 37 (3) (2021), 109838.

[90] S. Liu, T. Huynh, C.B. Stauft, T.T. Wang, B. Luan, Structure-function analysis of resistance to bamlanivimab by SARS-CoV-2 variants kappa, delta, and lambda, J. Chem. Inf. Model. 61 (10) (2021) 5133–5140.

[91] D. Benvenuto, F. Benedetti, A.B. Demir, M. Ciccozzi, D. Zella, Analysis of three mutations in italian strains of SARS-CoV-2: implications for pathogenesis, Chemotherapy 66 (1–2) (2021) 33–37.

[92] S. Pascarella, M. Ciccozzi, D. Zella, M. Bianchi, F. Benedetti, , et al.Benvenuto, SARS-CoV-2 B.1.617 Indian variants: are electrostatic potential changes responsible for a higher transmission rate? J. Med. Virol. 93 (12) (2021) 6551–6556.

[93] D.C. Groves, S.L. Rowland-Jones, A. Angyal, The D614G mutations in the SARS-CoV-2 spike protein: implications for viral infectivity, disease severity and vaccine design, Biochem. Biophys. Res. Commun. 538 (2021) 104–107.

[94] W.T. Yang, W.H. Huang, T.L. Liao, T.H. Hsiao, H.N. Chuang, P.Y. Liu, SARS-CoV-2 E484K mutation narrative review: epidemiology, immune escape, clinical implications, and future considerations, Infect.Drug Resist. 15 (2022) 373.

[95] S. Thakur, S. Sasi, S.G. Pillai, A. Nag, D. Shukla, R. Singhal, S. Phalke, G.S.K. Velu, SARS-CoV-2 mutations and their impact on diagnostics,therapeutics and vaccines, Front. Med. 9 (2022), 815389.

[96] F. Ali, A. Kasry, M. Amin, The new SARS-CoV-2 strain shows a stronger binding affinity to ACE2 due to N501Y mutant, Med. Drug Discov. 10 (2021) 100086.

[97] C. Laffeber, K. de Koning, R. Kanaar, J.H. Lebbink, Experimental evidence for enhanced receptor binding by rapidly spreading SARS-CoV-2 variants, J. Mol. Biol. 433 (15) (2021), 167058.

[98] H.G. Woo, M. Shah, Omicron: A Heavily Mutated SARS-CoV-2 Variant Exhibits Stronger Binding to ACE2 and Potently Escape Approved COVID-19 Therapeutic Antibodies, bioRxiv, 2021.

[99] K. Huang, Y. Zhang, X. Hui, Y. Zhao, W. Gong, T. Wang, et al., Q493K and Q498H substitutions in spike promote adaptation of SARS-CoV-2 in mice, EBioMedicine 67 (2021), 103381.

[100] F. Fratev, N501Y and K417N mutations in the spike protein of SARS-CoV-2 Alter the interactions with both hACE2 and human-derived antibody: a free energy of perturbation retrospective study, J. Chem. Inf. Model. 61 (12) (2021) 6079–6084.

[101] P.F. Souza, F.P. Mesquita, J.L. Amaral, P.G. Landim, K.R. Lima, M.B. Costa, et al., The spike glycoproteins of SARS-CoV-2: a review of how mutations of spike glycoproteins have driven the emergence of variants with high transmissibility and immune escape, Int. J. Biol. Macromol. 208 (2022) (2022) 105–125.

[102] A. Singh, G. Steinkellner, K. Köchl, K. Gruber, C.C. Gruber, Serine 477 plays a crucial role in the interaction of the SARS-CoV-2 spike protein with the human receptor ACE2, Sci. Reports 11 (1) (2021) 1–11.

[103] S. Kumar, T.S. Thambiraja, K. Karuppanan, G. Subramaniam, Omicron and Delta variant of SARS-CoV-2: a comparative computational study of spike protein, J. Med. Virol. 94 (4) (2022) 1641–1649.

[104] S.R. Kannan, A.N. Spratt, K. Sharma, H.S. Chand, S.N. Byrareddy, K. Singh, Omicron SARS-CoV-2 variant: unique features and their impact on pre-existing antibodies, J. Autoimmun. 126 (2022), 102779.

[105] L. Wang, G. Cheng, Sequence analysis of the emerging SARS-CoV-2 variant Omicron in South Africa, J. Med. Virology 94 (4) (2022) 1728–1733.